DEVELOPMENT OF ADHESIVELY BONDED GLASS FIBER REINFORCED POLYPROPYLENE / ALUMINUM BASED FIBER METAL LAMINATES (FMLs)

A Thesis Submitted to
the Graduate School of Engineering and Sciences of
İzmir Institute of Technology
in Partial Fulfillment of the Requirements for the Degree of

MASTER OF SCIENCE

in Mechanical Engineering

by
Ceren TÜRKDOĞAN

July 2019

İZMİR

We approve the thesis of **Ceren TÜRKDOĞAN**

Examining Committee Members:

Prof. Dr. Metin TANOĞLU
Department of Mechanical Engineering, İzmir Institute of Technology

Assoc. Prof. Dr. Engin AKTAŞ
Department of Civil Engineering, İzmir Institute of Technology

Assist. Prof. Dr. Levent AYDIN
Department of Mechanical Engineering, İzmir Katip Çelebi University

18 July 2019

Prof. Dr. Metin TANOĞLU
Supervisor, Department of Mechanical Engineering, İzmir Institute of Technology

Prof. Dr. Sedat AKKURT
Head of the Department of Mechanical Engineering

Prof. Dr. Aysun SOFUOĞLU
Dean of the Graduate School of Engineering and Sciences

ACKNOWLEDGMENTS

I would like to give my sincere thanks to my advisor, Prof. Metin TANOĞLU for his guidance, support, motivation and encouragement during my thesis.

I would like to thank to my labmates Mustafa AYDIN, Zeynep AY, Osman KARTAV, Yusuf Can UZ and Serkan KANGAL for their help, support and motivation.

I am especially grateful to my project mate, my close friend Hatice SANDALLI for her contribution, help and motivation.

I am also deeply grateful to Mehmet Deniz GÜNEŞ for his mentoring, invaluable contributions, motivation, support and patience during my whole thesis work.

Lastly but most importantly, I offer sincere thanks to my family for their motivation, support and patience during my study.

ABSTRACT

DEVELOPMENT OF ADHESIVELY BONDED GLASS FIBER REINFORCED POLYPROPYLENE / ALUMINUM BASED FIBER METAL LAMINATES (FMLs)

One of the most important steps during the production of adhesively bonded fiber metal laminates (FMLs) is adhesive bonding. In glass fiber reinforced polypropylene/aluminum laminates, it is very difficult to provide good bond strength. In order to solve this problem, applying various surface pre-treatments to the bonding surfaces prior to adhesively bonded is very important for good performance properties.

In the present study, glass fiber reinforced polypropylene (GFPP) composite plates were manufactured from ($\pm 45^0$) fabrics using hot press compression method.

Tensile, Charpy impact and flexural tests were performed to investigate the mechanical properties of the composites.

The produced GFPP plate and Al were used as the adherends and polyurethane-based film as adhesive in FMLs. While manufacturing FMLs, various surface modification techniques (silane and sandblasting pre-treatment) were applied to aluminum for good adhesion of GFPP and Al interface and their effect on the adhesive properties of GFPP/Al laminates were presented. The mechanical properties lap shear, and flexural strength and Mode-I fracture toughness of the adhesively bonded Al/GFPP laminates were investigated to evaluate the effects of surface treatments. Scanning electron microscope (SEM) was used to examine the fracture surfaces.

Single lap shear test showed that the adhesion of the GFPP/Al was improved by treatments of aluminum surfaces with silane and sandblasting. According to Mode-I fracture toughness values, silane treated specimens gave the best results. Based on the flexural test results, no significant change was observed in the flexural strength values of treated specimens compared to non-treated specimens.

ÖZET

ADHEZYONLA BİRLEŞTİRİLMİŞ CAM ELYAF TAKVİYELİ POLİPROPİLEN / ALÜMİNYUM ESASLI FİBER METAL LAMİNATLARIN (FML) GELİŞTİRİLMESİ

Yapıştırıcı kullanılarak üretilen fiber metal laminatların (FML'ler) üretimi sırasında en önemli adımlardan biri, yapıştırıcı ile bağlama aşamasıdır. Cam elyaf takviyeli polipropilen / alüminyum katmanlı yapılarda, iyi yapışma mukavemetini sağlamak oldukça zordur. Bu problemi çözmek için, çeşitli yüzey önişlemlerinin, yapışma yüzeylere uygulanması, iyi performans özellikleri açısından çok önemlidir.

Bu çalışmada, cam elyaf takviyeli polipropilen kompozit plakalar sıcak presleme yöntemi kullanılarak, $\pm 45^{0}$ fiber yönlenmesinde ve örgüsüz kumaşlardan üretilmiştir. Üretilen kompozit plakanın mekanik özelliklerini belirlemek için çekme ve eğme testleri uygulanmıştır. Kompozit plakanın darbe özellikleri ise charpy darbe testi ile belirlenmiştir.

Yapıştırıcı film kullanılarak üretilen FML yapılarda, üretilen CEPP plakası ve Al yapıştırılacak yüzeyler olarak seçilmiştir. FML'leri üretirken, CEPP ve Al arayüzünün iyi bir şekilde yapışması için alüminyuma çeşitli yüzey modifikasyon teknikleri (silan ile yüzey önişlemi ve kumlama yüzey önişlemi) uygulanmış ve bu tekniklerin CEPP / Al tabakalı yapıların yapışma özellikleri üzerindeki etkileri incelenmiştir. Bu etkileri değerlendirmek için yapıştırıcı ile bağlanmış Al/CEPP tabakalı yapılara tek bindirmeli kayma, eğme ve mod-I kırılma tokluğu testleri uygulanmıştır. Kayma testinden sonra oluşan kırılma yüzeylerini incelemek için taramalı elektron mikroskopu kullanılmıştır.

Tek bindirmeli kayma testi sonuçlarına göre, GFPP / Al yapılarının yapışma özelliklerinin, alüminyum yüzeylerin amino bazlı silan bağlayıcı ajanı ve kumlama ile işlenmesiyle geliştiği gözlemlenmiştir. Mode-I kırılma tokluğu değerlerine göre ise, silanla yüzey önişlemine tabi tutulmuş numuneler en iyi sonuçları vermiştir. Eğme testi sonuçlarına dayanarak, yüzeyleri önişleme tabi tutulmuş numunelerin eğme dayanımı değerlerinde, işlenmemiş numunelere göre önemli bir değişiklik gözlenmemiştir.

TABLE OF CONTENTS

LIST OF FIGURES

Figure **Page**

Figure **Page**

LIST OF TABLES

Table **Page**

CHAPTER 1

INTRODUCTION

In recent years, there are many researches about to develop new materials with good properties of both composites and metals. Hybrid design is an arising process of joining metals and composites with desirable and original material properties such as low weight, higher stiffness and strength, high fatigue performance, resistance to damage of physical and radiation and design sophistication (Pramanik et al. 2017).As a result, in laminated structures with composite materials and metals, while the mechanical properties increase, the weight decreases(Kleffel and Drummer 2017).

Thermoplastic-based fiber metal laminated hybrid structures are being increasingly used in the automotive and aerospace industries. They used in military and commercial transport vehicles (Ochoa-Putman and Vaidya 2011). Thermoplastic-based laminates are more preferred than thermoset-based ones due to their fast production times, reformable nature, high recyclability, low cost, and volatility. Other benefits are the facility to reshape components, easy repairability, perfect energy-absorbing properties, and high impact strength (Cantwell 2000).

In real life, recent attention has focused on fiber reinforced thermoplastic (FRP) composites although FRP is more expensive than major metals. But glass fibers are relatively cheap compared with carbon and aramid fibers, so that glass fiber reinforced plastics (GFRP) are more widely used in the industry (Matsuzaki, et al. 2008).

In the aerospace and automotive industry, fiber-reinforced polymers have been used to reduce the weight for many years. Recently, glass fiber reinforced polypropylene (GFPP) has come to the forefront for many engineering applications due to it has a good balance between properties and costs(Reyes and Kang 2007).

In recent years, metal/thermoplastic polymer based laminated structures like steel or aluminum/fiber reinforced PP laminate have gained attention due to good mechanical properties. However, in such of FMLs, to obtain good adhesion strength is an important problem (Chen, et al. 2007).

Since polypropylene is mostly hydrophobic, has low surface free energy, and it has a poor chemical interaction therefore, fiber reinforced polypropylene joints have

poor bonding strength. The crucial point in the development of such fiber metal laminated hybrid structures is the interfacial bonding between the different layers of the laminate (Astigarraga et al. 2019).

In fiber/metal laminated structures, classic joining techniques (i.e. riveting, clinching, and mechanical fastening) are hardly feasible on composite materials because they create stresses at the joint area. Furthermore, for fiber reinforced polymer structures, a drilling process breaks the fibers, causing several damages. These damages cause a decrease in mechanical properties such as fatigue strength of joint area (Valenza, et al. 2011). Therefore adhesive bonding has become popular over the last decade as it has the unique opportunities to reduce weight, increase the fatigue life of joints, have better environmental resistance and ensure the bonding of different materials in hybrid structures (Astigarraga et al. 2019).

In the process of adhesive bonding, surface pre-treatment is a very important step. Surface treatments can be applied to both thermoplastic and metal surface to increase the bonding strength. In literature, some surface treatment techniques for PP are as follows; chemical etching, flame treatment, surface grafting, electron beam and microwave irradiation, plasma discharge as corona discharge and etc. The aim of these treatment techniques primarily at obtaining polar groups on polymer surfaces, in this manner increasing the values of surface free energy and developing adhesive ability of the polymeric materials (Chen, et al.2007) . Similarly, surface treatment of the metal is used to enhance the bonding characteristics. Metal surface is treated by mechanical, chemical, electrochemical, etc. (Sinmazçelik et al. 2011).

Shimamoto, et al. (2016). investigated the effect of chemical and mechanical surface modification of aluminum on Al/GFPP hybrid structures bonding strength. The results of the experiment show that the best result is chemical etching compared to the sand blasting. Also, they indicated that the chemical etching depth does not influence the bonding strength

Cantwell (2000) examined the effect of chemical etching (chromate coating for Al alloy) and a maleic anhydride modified polypropylene layer at the glass fiber reinforced polypropylene and aluminum alloy interface. From the results, excellent adhesion was seen incorporation of a maleic-anhydride modified PP interlayer.

The aim of this study is manufacture glass fiber reinforced polypropylene and aluminum fiber-metal laminates by using adhesive film successfully and improve the

adhesive properties of this fiber metal laminates with using different pre-treatment techniques such chemical etching and sandblasting methods.

CHAPTER 2

FIBER COMPOSITE-METAL HYBRID STRUCTURES

2.1. Fiber Composite-Metal Laminates

Over the last 20 years, fiber composite-metal laminates have gained attention in many engineering applications. There are many searches for lightweight materials that can replace the conventional aluminum alloys with similar or better properties. FMLs material systems consisting of thin metal and fiber reinforced polymer-matrix composite show superior strength, fatigue and stiffness properties of composites as well as the properties of metals such as machinability and toughness (Reyes and Kang 2007). They used for structural aerospace applications such as aircraft fuselage, lower wing skins and interior materials of airplanes. Valenza, et al. (2011) examined the mechanical properties of the GFPP/Al laminated (FMLs) structures for the aviation industry.

Fiber composite metal laminates are consisting of separate metallic and composite layers that are usually bonded using adhesives and they have both advantages of fiber composite and metallic materials (Zal et al. 2017). Fiber composite metal laminates are schematically shown in Fig.2.1.

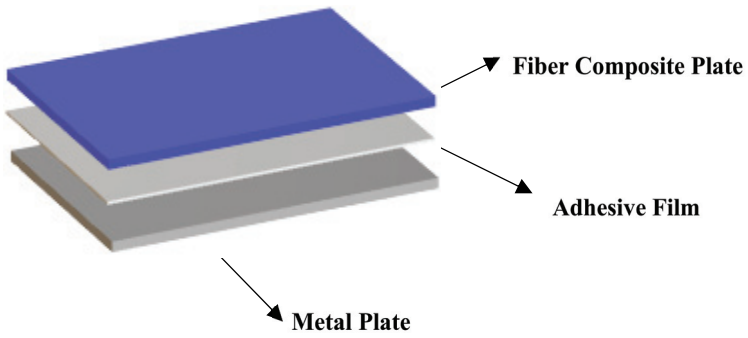

Figure 2.1. Schematic representation of FMLs

The early produced polymer-metal laminated hybrid structures, for use in the aerospace industry were form on epoxy thermosetting polymers. But nowadays, thermoplastic based composite laminates are more preferred than thermosetting based

ones. Because thermosetting-based composites are generally brittle and the production process is long-term. Thermoplastic based fiber composite-metal laminates have higher toughness, short process cycle times and low-cost production. In addition, the low volatility, and high recyclability of thermoplastics are very important characteristics for vehicle industry. Thermoplastics, especially polypropylene has become attractive because of its features such as low density and low cost (Reyes and Kang 2007).

In many applications, the use of fiber reinforcement in the polymer matrix has been found to provide superior durability to the material to be produced. Fiber-reinforced composite materials comprise of matrix and fibers embedded in a matrix. While the fibers carry the main load with high strength and modulus, the matrix transfers the stress between the fibers and protects the fiber surface from the mechanical effects (Etcheverry and Barbosa 2012).

The glass fiber polypropylene (GFPP) is one of the most widely used fiber reinforced thermoplastic based composites. GFPP is preferred in building construction, marine, aeronautical applications and automotive industries etc. Since PP has a hydrophobic structure, bonding structure and surface treatment have become very important in metal-composite hybrid laminates to produce well-adhering structures (Ostapiuk, et al. 2014). Abdullah, et al. (2015) studied on interfacial fracture of fiber-reinforced thermoplastic/metal laminates. They used two different fiber reinforced thermoplastics when manufacturing fiber metal laminates. One is self-reinforced PP and the other is glass fiber-reinforced PP. They compared the mechanical test results of these two different based FMLs.

2.2. Adhesive Joining Method

It is expected that metal-composite materials (FMLs) will be used more widely in the future due to their good results in terms of strength and fracture toughness and low weight. In general, the joining of polymeric materials to dissimilar materials is becoming more widely and significant in aerospace industry. They are in search high-applicability and faster assembly methods and excellent corrosion resistant, more tough and lightweight products (Berry and Namkanisorn 2005) . With this aim, Cerny and Morscher (2006) and Molitor and Young (2002) investigated the durability of

adhesives in the interface polymer composite–metal bond, using titanium alloy and fiber glass reinforced polymeric composite as substrate .

The traditional joining techniques for fiber reinforced polymeric composite-metal (FMLs) laminates contain mechanical fastening, adhesive bonding and welding (Messler 2000). The good performance of the fiber metal laminates depends on the good joining of the structure because the joints are always potential location of damage initiation. The interface strength between composites and metallic materials is the main subject to be developed. To ensure a reliable load carrying at low weight, the correct joining technique should be selected. Therefore, creating a high-strength interface between FRP and metallic parts is a significant technology (Tang and Liu 2018).

The adhesive joining method has become more attractive than mechanical bonding because of its low weight and cost, its simplicity of use and allow for uniform load distributions (Huang, et al. 2014).

In order to bond the components, the adhesive bonding process is very important for durable structures. This process is used to produce structures that are complex in shape, which cannot be produced in one piece. Adhesive bonding makes possible joining dissimilar materials without damage to the main structures. For example, in fastening joining technique, fastener holes break the fibers and it causes regional damage which leads to a decrease in strength in the structure. But this is not observed in the adhesive bonding technique. This is just one of the advantages of the adhesive bonding technique (Ribeiro et al. 2016). Other advantages of the adhesive joining method are providing to materials reduction of weight, more uniform load transfer, and cost-saving, improved damage tolerance. Due to such advantages adhesive bonding process has been used in variety applications such as electronics, aeronautical industries (on F-18 bonded wings), automotive industries and etc. (Sinmazçelik et al. 2011)

Due to the fact that adhesive bonding in thin layers is easy to apply, this joining technique is very suitable for the production of ultra-light fiber reinforced composite-metal hybrid structures (Huang, et al. 2014) . Besides, in some cases adhesive joining technique is the best way, such as in thin-walled structures with large thickness changing (Rudawska 2010). Taib et al. (2006)investigated the other bonding techniques such as bolts and rivets increase the high stress concentration at the joint area. This situation results in a decrease in the mechanical properties of adhesive bonded structures.

Polypropylene (PP) and other polyolefins have been used as adherend in many adhesive bonding industrial applications. Nowadays, fiber-reinforced PP has attracted attention to produce of ultra lightweight and strength fiber composite-metal hybrid structures. However, since PP has a hydrophobic structure it has poor bondability property to other materials. This limited the use of PP and other polyolefins in the production of the joining process (Chen, et al. 2007). In many studies, in order to overcome like these problems, effective surface treatment techniques are performed the adherend surface in FMLs structures (Green, et al. 2002). In adhesive bonding, surface treatment before the bonding process is the most crucial step (Park et al. 2010). Both composite and metal surfaces can be specially treated before the adhesive bonding process in the fiber reinforced composite/metal hybrid structures. Because surface pre-treatments significantly improve the strength of the adhesive joints and affects the failure mechanism that will occur. With surface treatment, properties of adhesion surface such as surface cleaning, wettability, surface roughness and polarity are changed and well-adhered structures are obtained (Critchlow and Brewis 1996).

2.3. Surface Treatment Methods

In fiber composite/metal hybrid structures, most important step for an adhesive bonding is surface treatment. Effective surface treatment methods allow a durable and strong joint area between the fiber composites and metals.

There are many researches about to improve the surface free energy of polypropylene with surface treatment methods and the purpose of these studies is creating a surface with high bondability and wettability, developing alternate interface including copolymers, grafting, also increasing the quantity of bond sites (Guild et al. 2008).

Surface treatment methods of polymers and metallic materials are diverse. There are many methods for treating the metallic alloys and polymers that including mechanical, chemical, electrochemical, thermal, plasma, laser, coupling agent treatments etc. (Sinmazçelik et al. 2011). For example, the simplest way of aluminum alloy pre-treatments are based on, vapour degreasing, solvent wiping or mechanical abrading (Valenza, et al. 2011).

Surface treatment prior to bonding generally increases the bonding strength by increasing surface tension and surface roughness or changing surface chemistry.

In mechanical treatment, the surface area is increased and surfaces with different degrees roughness are obtained. This allows the adhesive to penetrate into the structure more easily and increase the bonding area thus providing better mechanical bonding. Furthermore, the oxide layer on the surface of the bonding area can be removed easily by mechanical treatment (Sinmazçelik et al. 2011).

In adhesive bonding, achieving chemically active surface is essential. This surface can be generated by acid etching treatment. Acid etching process provides to FMLs more durable bonded (Valenza, et al. 2011). Acid etching can be divided into three main categories to improve the metallic surfaces: chromic–sulphuric acid (CAE), Forest Product Laboratory (FPL), and sulfo-ferric acid etches. Chromic-sulphuric acid (CAE) etching is the most widely applied chemical treatment for metals, and especially for aluminum alloys (Sinmazçelik et al. 2011).

Leena et al. (2016) applied three different chemical surface treatment methods to the surface of the aluminum alloy, including solvent cleaning, FPL etching and priming using an epoxy based primer and compared test results of their surface properties. This study showed that FPL etching treatment gave the best results in terms of surface energy, surface roughness and joint strength (Leena et al. 2016).

On some surfaces where there is corrosion, chromic-sulfuric acid etching is inefficient. Therefore, after the etching of the sulfuric acid, the aluminum surface can be prevented from corrosion if anodized before bonding. Anodizing process is very important for the aerospace industry, since this process ensures optimum strength and permanent adhesive bonding (Sinmazçelik et al. 2011).

Correia, et al. (2018) studied four types of chemical surface treatment for Al alloy, being them the Phosphoric Acid Anodizing (PAA), the Chromic Acid Anodizing (CAA), the Sulfuric Acid Anodizing (SAA) and the Boric-Sulfuric Acid Anodizing (BSAA). They obtained SAA surface treatment results 8% better than others. According to some studies, PAA has better joint durability compared with the CAA.

Etching of Al surface with acid, give enhanced performance compared to physical treatment methods but acid etching process is highly toxic and corrosive. Chromic or phosphoric acid anodizing is more effective in relation to the durability. However, anodising is a complex multistage process and its applicability is a very difficult. Due to these disadvantages, it has become common to use coupling materials

such as silanes or sol-gels to bond between the polymer and the metal surfaces and to form a hydrophobic interface (Berry and Namkanisorn 2005).

2.3.1. Chemical Surface Treatment with Silane Coupling Agents

Surface pre-treatment with silane coupling agents of metal surfaces prior to bonding, can be improved adhesion characteristics bonded surface area of between distinct materials such as inorganic glasses and metals. Polymer-metal adhesion is improved by using silane coupling agents which produce covalent bonds in the interface, thus increasing the adhesion strength and durability. Also, silane treatments are used to make the surface from hydrophobic to hydrophilic in order to increase surface wetting properties (J. G. Kim et al. 2010). Silane is applied by dipping the metal in the diluted solution or by coating a thin layer on the metal surface after that cured at elevated temperature. Normally a silane is made up in a dilute solution, applied as a thin coat onto the surface by dipping the aluminum or painting the silane, and then cured at elevated temperature onto the surface.

Table 2.1. Different types of silane coupling agents

Typical Silane Coupling Agents		
Abbreviation	**Name**	**Structure**
APMDES	aminopropyl methydiethoxysilane	$H_2N(CH_2)_3Si(OC_2H_5)_2$
APTES	3-aminopropyltriethoxysilane	$H_2N(CH_2)_3Si(OC_2H_5)_3$
APMDMOS	(3-acryloxypropyl) methydimethoxysilane	$CH_2=CHCOO(CH_2)_3(CH_3)Si(OCH_3)_2$
GPTMOS	3-glycidoxypropyltrimethoxysilane	$CH_2(O)CHCH_2O(CH_2)_3Si(OCH_3)_3$
DDS	dimethyldichlorosilane	$(CH_3)_2SiCl_2$
MPTS	mercaptopropyl triethoxysilane	$SH(CH_2)_3Si(OC_2H_5)_3$
PTMS	phenyltrimethoxysilane	$PhSi(OCH_3)_3$
VTES	vinyltriethoxysilane	$CH_2=CHSi(OC_2H_5)_3$

In literature, silane coupling agents denoted as $RSiX_3$. In here R represented by organofunctional radicals. Those radicals are non-hydrolyzable and selected to react with to resin in the organic part, and the X groups are hydrolyzable alkoxy groups that connect with the inorganic surface. There are many silane coupling agents, and they differ from each other in terms of their reactivity degree. Table 2.1 shows the name and

structures of different types of silane coupling agents. According to Table 2.1, silanes may be generated with, amine, epoxy, and other functionalities (Rafiq et al. 2011).

Honkanen et al. (2009) used amino silane as a coupling agent between thermoplastic urethane and stainless steel. They examined the effect of silane surface treatment parameters (i.e. silane concentration, etc.) and related it to the adhesion properties.

In silane application, the thin film obtained on the surface is produced from the dilute aqueous solution of a silane coupling agent. This film is formed by a series of hydrolysis and condensation reactions between the silane solution and the adherend surface. The organic part of the silane is selected to react with the polymeric resin. In between the metal and polymer, polymeric network is formed by the self-condensation cross-linking process. The high bond strength and durability provided by the silane coupling agents is the presence of covalent bonds. This bond between a metal surface and hydroxyl groups of the silane is called Fe–O–Si bonds (W. S. Kim and Lee 2007). These reactions are shown in Fig. 2.2.

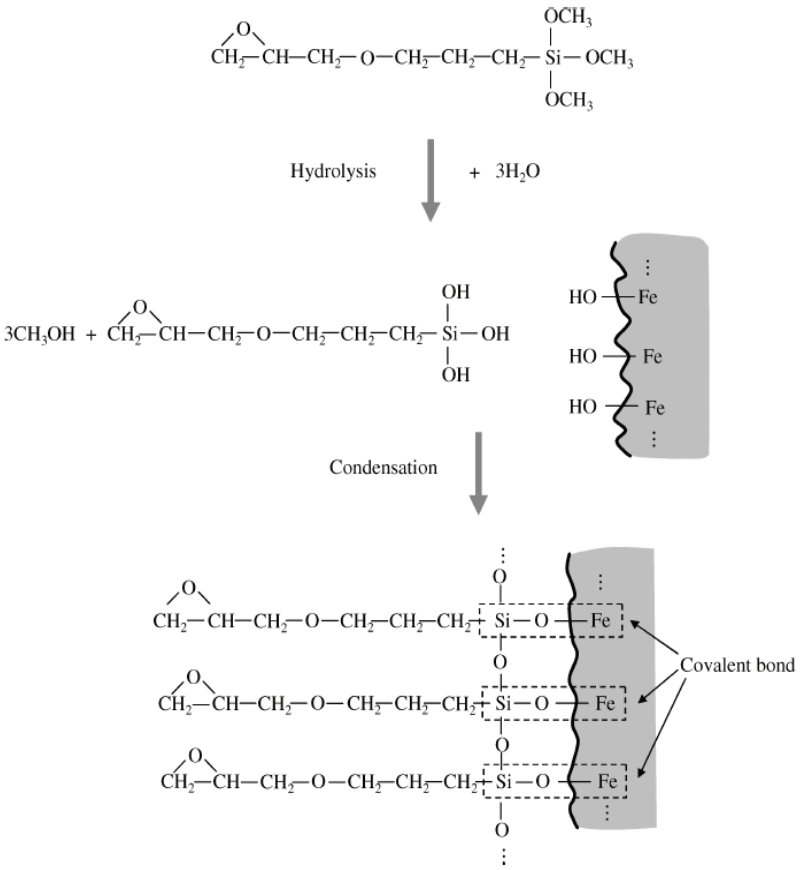

Figure 2.2. Scheme of γ-glycidoxypropyltrimethoxysilane hydrolysis and condensation reactions (Source: Kim and Lee, 2007)

In literature there are many studies about using silane coupling agents for surface treatments. Kim et al. (2012) investigated the optimum conditions for silane pre-treatment for the adhesively bonded aluminum structures at the cryogenic temperature to obtain high bond strength. In their work, as a silane coupling agent, γ-glycidoxypropyltrimethoxysilane (γ -GPS), was applied on the aluminum adherends at the cryogenic environment (Kim et al. 2010). Valenza, et al. (2011) used the, γ-glycidoxypropyltrimethoxysilane (γ- GPS) silane coupling agents to increase the adhesion strength between aluminium and a glass fiber reinforced polymer.

2.3.2. Sandblasting Surface Treatment

Sandblasting is which one of the most common used mechanical treatment technique for metals. The roughened metal surface can improve the bonding strength with mechanical interlocking effect. In this surface treatment method, sample surfaces are roughened by the effect of grit, which is accelerated by pressure of air (Shimamoto, et al. 2016).

Sandblasting surface treatment changes the bonding surface topography and chemical stability of adherend by peak-and-valley type morphology (Sinmazçelik et al. 2011).

In the literature, there are studies to investigate the effect of sandblasting surface treatment on metal surface. Shimamoto, et al. (2016) used glass fiber reinforced polypropylene and aluminum alloy A6061 as adherend in the fiber metal laminates. They applied sandblasting and chemical etching surface treatment to the aluminum surface and compared the effect of these surface pre-treatment methods on GFPP and Al joint surface.

Spaggiari and Dragoni (2013) examined the effect of mechanical surface treatments on the strength of adhesive bonded joints. They applied different mechanical surface treatments such as sandpapering, sandblasting, and knurling to the specimens. As a result of experiments, sandblasting was determined as the best mechanical surface treatment since it caused cohesive failure, and it gave more stable and repeatable results for metallic adherends to be bonded.

According to Gadelmawla et al. (2002), finding surface treatment parameters after the applying surface treatment is a very important step. In this study, surface

treatment parameters are defined as follows: the arithmetic average height parameter (R_a), is the defined as the average absolute deviation of the roughness irregularities from the mean line over one sampling length as shown in Figure 2.3. The ten point height (Rz), is described as the height difference between the average of the five highest peaks and five lowest valleys as shown in Fig. 2.4.

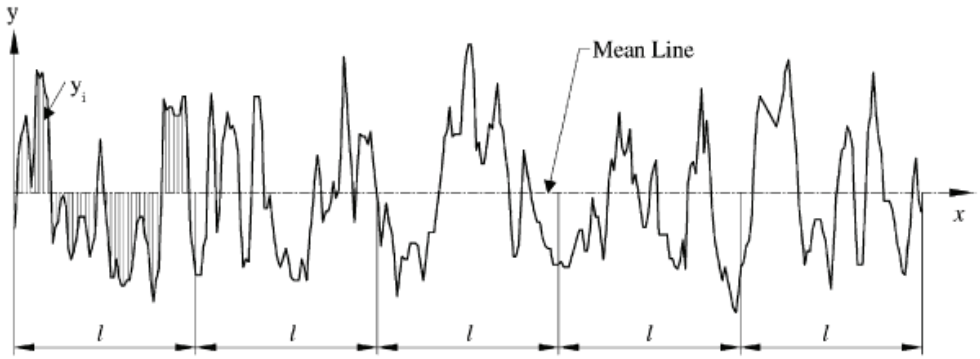

Figure 2.3. Definition of the arithmetic average height (Ra) (Source: Gadelmawla et al.,2002)

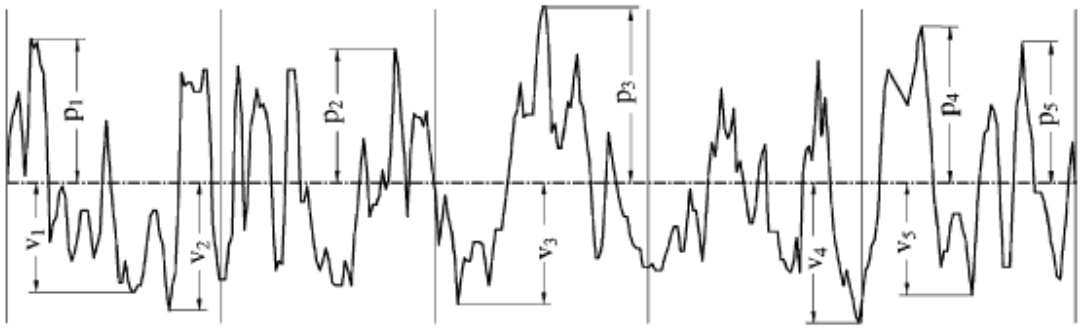

Figure 2.4. Definition of the ten point height parameter (Rz) (Source: Gadelmawla et al., 2002)

2.4. Failure in Adhesive Bonded Joints

In adhesively bonded joints, generally two different failure mechanisms are occurred. These failure mechanisms are called as cohesive and adhesive failure. Adhesive failure is interfacial failure and it happens among the adhesive and one of the adherends. It usually occurs in adhesive bonded structures with poor bonding. Cohesive failure can be explained by the fact that the adhesive layer remains on both adherend surfaces, and seldomly, when the adherend fails before the adhesive fails, with division

taking place entirely within one of the adherends. Fig. 2.5 shows different types of failure in adhesive bonded joints schematically (Messler 2004).

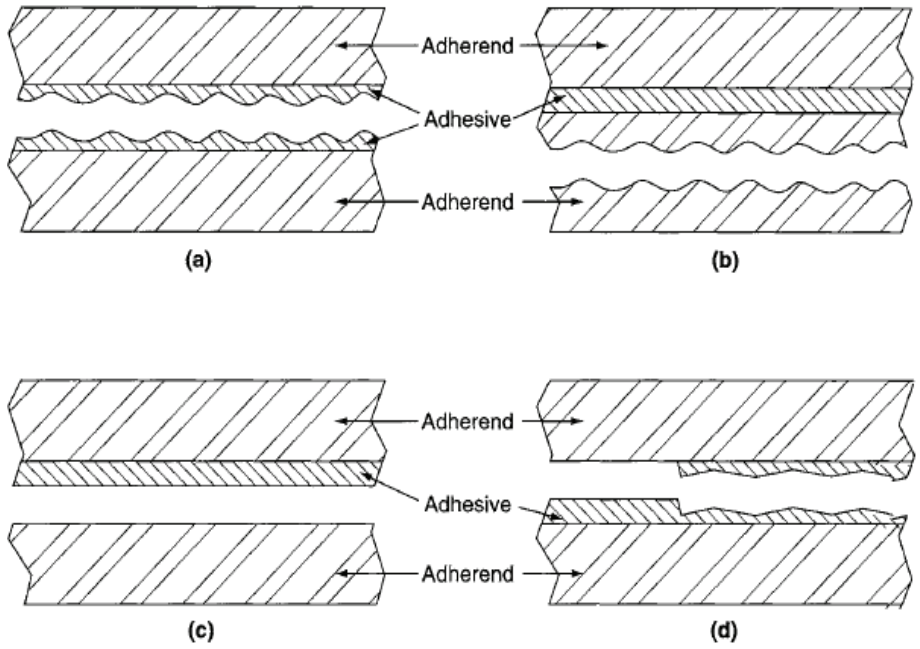

Figure 2.5. Scheme of cohesive and adhesive failure in adhesive bonded joints, (a) cohesive failure within the adhesive and (b) cohesive failure within one of the adherends, (c) adhesive failure throughout the adhesive-adherend interface (d) mixed-mode failure. (Source: Messler, 2004)

De Freitas and Sinke (2014) studied to improve the adhesion capability of adhesively bonded aluminum-composite joints. They accomplished that in adhesively bonded structures the failure mode is more crucial than the failure load; furthermore, they showed that the surface treatment of adherends is very important for well adhering structures.

In real life, joint failure is usually a mixture of adhesive and cohesive failure. In joint surface, failure mode is generally indicated as a percentage of adhesive or cohesive failure. A failure in adhesive bonded structures must be 100% cohesive to be ideal (Messler 2004).

Correia, et al. (2018) investigated the effect of different surface treatment on adhesively bonded aluminum-aluminum joints. They applied to specimens two different electrochemical surface treatments and performed the single lap shear test to specimens. Based on, examination of joint surfaces of single lap shear test specimens they obtained the adhesive failure and mixture of adhesive and cohesive failure.

Goushegir (2015) studied the effect of various aluminum surface pre-treatments on metal composite bonding surface. In this study, Al as metal adherend, CF-PPS is also selected as fiber composite adherend. They applied the mechanical, chemical and electrochemical surface pre-treatments to their Al adherends. According to the results of the fracture surface analysis of the study, in the specimens prepared with all surface pretreatments except phosphoric acid anodizing + primer (PAA-P) surface tretment, the failure occurs in the composite at the center of the joint because a PPS layer can be defined on the aluminum side.

2.5. Test Methods to Evaluate Mechanical Properties of Adhesively Bonded Fiber Metal Laminates

Analysis of adhesively bonded joints can be realized by some mechanical tests. For adhesive structural joints, strength can be determined using lap shear tests, toughness can be determined with double cantilever test.

2.5.1. Single Lap Shear test

In order to evaluate the shear strength of the joints and quantify adhesive bond durability single-lap shear test can be applied to the adhesive bonded structures. Also, single lap shear tests can be performed to determine adhesive bonded both similar and dissimilar materials shear strength (Molitor and Young 2002).

In lap shear test, tension is performed throughout specimens length and due to tension in the joint region, the adhesive is subjected to shear stress. In Fig. 2.6 the lap shear test is schematically shown.

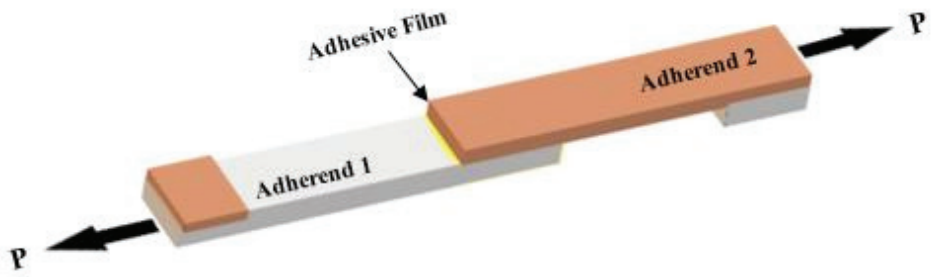

Figure 2.6. Schematic of lap shear test specimen under tensile loading

In literature, in order to examine the bonding characteristics of adhesive for joining materials, some lap shear test methods are defined. Some of these standards are as follows; for joining plastics ASTM D 3163 (Standard Test Method for Determining Strength of Adhesively Bonded Rigid Plastic Lap-Shear Joints in Shear by Tension Loading) ,for joining metals ASTM D 1002 (Standard Test Method for Apparent Shear Strength of Single-Lap-Joint Adhesively Bonded Metal Specimens by Tension Loading), and for joining fiber reinforced plastics to metals and to themselves ASTM D 5868 – 01(Standard Test Method for Lap Shear Adhesion for Fiber Reinforced Plastic Bonding)

Valenza, et al. (2011) studied about mechanical behaviour of GFPP/ Al fiber metal laminates. They applied the lap shear test to determine the shear strength at the adhesive joint area of between the metal and the composite according to ASTM D1002.

Molitor and Young (2002) investigated the characteristics of adhesive bonding of a titanium alloy/glass fibre reinforced composite materials. They performed some mechanical tests to specimens. They applied the single lap shear test according to ASTM D 5868-95 test aim to determine durability assessment of the specimens.

2.5.2. Double Cantilever Beam (DCB) test

The Mode-I interlaminar fracture toughness of the samples was determined by double cantilever beam (DCB) experiments. DCB test is generally used for determining initiation and propagation values of Mode I fracture energy under loading.

In DCB test, load is applied to samples with the same crosshead speed in opposite directions (i.e. tensile load) and is applied to a DCB specimen with an embedded through-width insert at the specimen mid-plane (Broughton 2012) (Fig 2.7).The crack tip progression in a DCB specimen can be observed with a CCD camera, a microscope or a crack gauge. At the end of the test, the critical energy release rate was determined as a function of the crack length (Shimamoto, et al 2016).

ASTM D5528-13 standard is used in order to investigate mode-I interlaminar fracture toughness of fiber-reinforced polymer matrix composites. According to ASTM D5528-13 standard, there are three data reduction methods to calculate the G_{Ic} values. These are, a compliance calibration method (CC), modified compliance calibration method (MCC) and modified beam theory (MBT). The MBT method is the

recommended method for calculating the G_{Ic} values because it gives more conservative results (ASTM-American Society for Testing and Materials 2001).

Figure 2.7. Schematic of DCB test specimen under tensile loading

2.5.3. Three Point Bending Test

Flexural properties of material can be determined by using the three point bending test.

In three point bending test, load is applied to the middle of a test specimen. The upper surface of the specimen is in compression and bottom surface is in tension. Force and displacement values are obtained during the test. The flexural strength, modulus and flexural strain of specimens are calculated from the data taken three point bending test. Three point bending test setup is schematically shown in Figure 2.8.

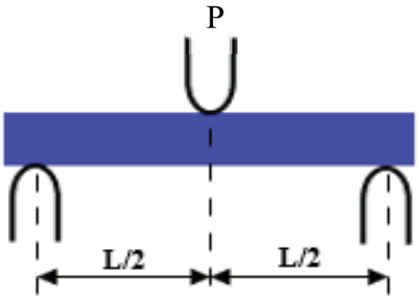

Figure 2.8. Schematic of flexural test setup

There are two ASTM standards to determine the flexural properties of reinforced and unreinforced plastics materials. The dimensions of the test specimen are specified in

these standards. One of these standards is ASTM D 790 (Standard Test Methods for Flexural Properties of Unreinforced and Reinforced Plastics and Electrical Insulating Materials) and the other one is ASTM D 6272 (Test Method for Flexural Properties of Unreinforced and Reinforced Plastics and Electrical Insulating Materials by Four-Point Bending.)

CHAPTER 3

EXPERIMENTAL

3.1. Materials

In this study, the fiber/metal laminated structures were manufactured using non-crimp ($\pm 45^0$ biaxial glass) glass fiber polypropylene fabrics (GFPP) as a thermoplastic based composite layer and 2 mm thick aluminum as a metal layer. Biaxial non-crimp GFPP fabrics used in the study.

For aluminum surface treatment silanol solution which was prepared by silane coupling agent Z-6032 from XIAMETER OFS, glacial acetic acid and pure water was used. The chemical structure of the silane used is shown in Fig.3.1 This silane coupling agents contain a vinylbenzyl and amine organic and a trimethoxysilyl inorganic group.

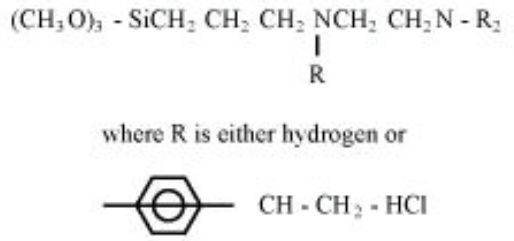

Figure 3.1. Chemical structure of XIAMETER OFS-6032 Silane (Source: Dow Corning (2017) XIAMETER® OFS-6032 Silane Product data sheet)

A polyurethane based adhesive film (Bemis 3218) was provided from Bemis Associates Inc., USA. General properties of Bemis 3218 are glue line temperature is 120 ^{0}C to 130 ^{0}C and pressure is 2.8 to 4.2 Bar.

3.2. Thermoplastic Based Composite Plate Manufacturing

Glass fiber reinforced polypropylene composite plate manufactured from glass fiber/PP non-crimp fabrics by using hot press compression molding machine.

The thermoplastic based composite plate was manufactured following the steps below respectively:

- 6 layers of (±45°) glass fiber polypropylene non-crimp fabrics were cut into mold dimensions and placed in a mold.
- The mold was transferred to hot press machine.
- The pressure was applied to GFPP fabrics until the temperature of the press reaches the lamination temperature. The process temperature was determined to be 200 ^{0}C. The pressure value was determined as 0.7 MPa.
- The heating system of the hot press, after reaching the desired temperature, it was kept at this temperature for 45 minutes and was turned off.
- Finally, glass fiber reinforced polypropylene plate was produced and removal from the mold.

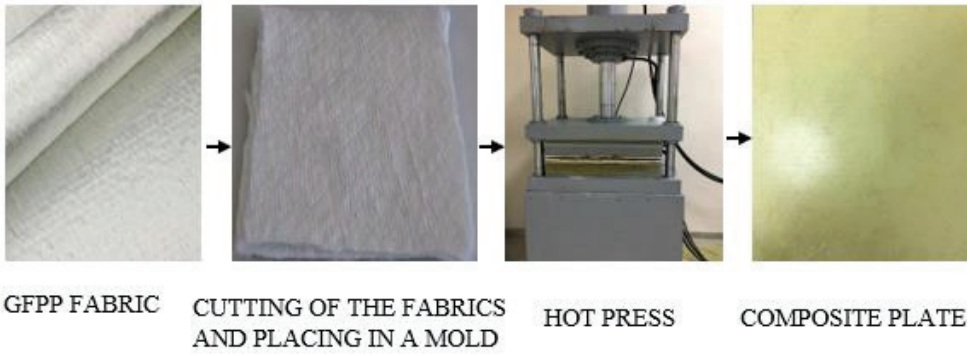

Figure 3.2. Composite plate manufacturing procedure

3.2.1. Characterization of GFPP Plate

3.2.1.1. Mechanical Property Characterization

3.2.1.1.1. Tensile Test

Tensile strength, strain and modulus of specimens were calculated with using tensile test.

Test specimens were prepared according to ASTM D 3039M-93 test standard and 5 specimens were cut from GFPP composite plates with dimensions of 250 mm length and 25 mm width. Tensile test was applied to specimens at room temperature

using Shimadzu AG-IC Universal Test Machine with 100 kN capacity load cell and at a cross head speed of 2 mm/min. The displacement values were obtained using video extensometer. The tensile test set up is shown in Figure 3.3.

Figure 3.3. Tensile test specimen during test

3.2.1.1.2. Three Point Bending Test

Three point bending test samples prepared according to ASTM D790 test standard. Flexural properties of GFPP composite and load-displacement curves were obtained from the three point bending test. Test was carried out using Schimadzu™ universal test machine and, a crosshead speed of test machine is set to 2 mm/min. Test specimens were sectioned using diamond saw with 10 mm in width, 3 mm in height. Length of specimens were related to span ratio, and span to thickness ratio was selected as 16. Three point bending test set up is shown in Figure 3.4.

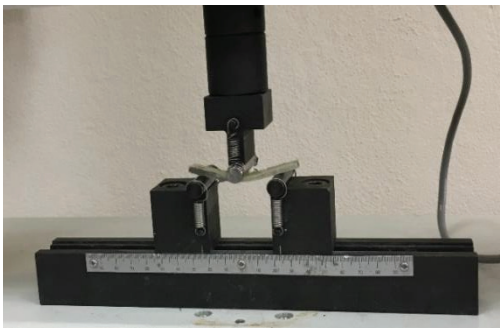

Figure 3.4. Flexural test specimen during test

Flexural stress, strain and modulus values were calculated based on equations below. In order to determine flexural stress Equation 3.1 was used.

$$\sigma_f = \frac{3PL}{2bd^2} \tag{3.1}$$

In equation 3.1 , σ_f is the stress in outer fibers at midpoint, P is load, L is support span length, b is width and d is thickness of the specimen tested. Flexural strain was calculated using Equation 3.2.

$$\varepsilon_f = \frac{6Dd}{L^2} \tag{3.2}$$

where, εf is flexural strain, D is maximum deflection of the center of beam, d is thickness of the specimen and L is support span length. Equation 3.7 was used to determine the flexural modulus.

$$E_b = \frac{L^3 m}{4bd^3} \tag{3.3}$$

where, E_b is flexural modulus of elasticity, L is support span length, b is width and d is thickness of the specimen, m is slope of the tangent to the initial straigh-line portion of the load deflection curve.

3.2.1.1.3. Charpy Impact Test

Charpy impact test carried out based on ISO 179-1 test standard. At least 6 specimens with a length of 80 mm, a thickness of about 4 mm and a width of 10 mm were tested to determine the Charpy impact energy of GFPP plate during fracture. This test method also gives information about the toughness of GFPP.

Charpy Impact Test is also known as Charpy V-notch Impact Test. In Charpy Impact test, firstly 2 mm depth ‘V’ shape notch was made to samples by notch opening apparatus. This test apparatus (CEAST Resil Impactor, Corporate Consulting, Service & Instruments, Inc.) for making V-notch impact test are shown in Figure 3.5.

Figure 3.5. Charpy test specimen during test

The specimen is positioned at the base of test apparatus. The load is applied as an impact from a pendulum hammer that is released from a fixed height. During the release of the pendulum, the sample is impacted and broken at the notch. As the pendulum continues to swing, it reaches the maximum height and this height is lower than the initial height. The energy absorption is determined from the difference between the maximum height reached by the pendulum and the first height (Callister and Rethwisch 2007).

3.2.1.2. Thermal Property Characterization of GFPP

3.2.1.2.1. Differential Scanning Calorimetry (DSC)

DSC is the most widely used thermoanalytical techniques for polymer materials. Although DSC is used to characterize mainly polymers, it can also be used in the characterization of organic materials and inorganic materials such as metals and ceramics.

Temperatures and heat flows in the transition of materials can be measured by DSC as a function of temperature and time.

In this study, in order to determine the melting temperature of glass fiber polypropylene DSC thermoanalytical method was used. 4-6 mg of polypropylene samples were prepared and thermoanalytical measurements were performed with TA

Instrument Q10. The DSC measurements were performed at a constant heat rate of 2°C/min from room temperature to 200°C.

3.3 Manufacturing of GFPP/Al Hybrid Structures

After manufacturing of GFPP plate, GFPP and 2 mm thick aluminum plates were bonded with temperature and pressure using adhesive film. Surface treatments were applied to GFPP and aluminum plates in order to improve the bondability properties of the joint surfaces of fiber metal laminates. Manufactured GFPP/Al laminated structure is schematically shown in Figure 3.6.

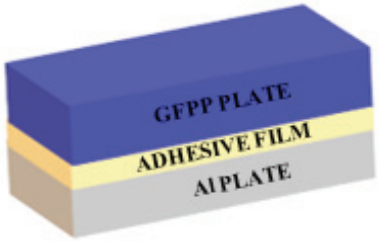

Figure 3.6. Scheme of GFPP/Al laminated structure

The process steps of the manufacturing of GFPP/Al (fiber/metal laminates) structures are as follows:

3.3.1. Surface Treatments of Aluminum

In this study, two different aluminum surface treatment methods are used which aim to improve bonding properties of the surface between aluminum and composite interface. They are listed Table 3.1. For each test non-treat samples were prepared as reference samples to compare the results of the different surface treatments.

Table 3.1. Various aluminum surface pre-treatments used in present study

CATEGORY	SURFACE PRE-TREATMENT	SYMBOL
As-received	Nontreated	NT
Mechanical	Sandblasting	SB
Chemical	Etching with Silane Coupling Agent	ST

In order to chemical treat the aluminum surface, silanol solution was prepared using distilled water, glacial acetic acid and silane.

Silane treatment was applied to aluminum surface according to product information of XIAMETER OFS Z-6032 silane. The surface modification with silane is schematically illustrated in Figure 3.7.

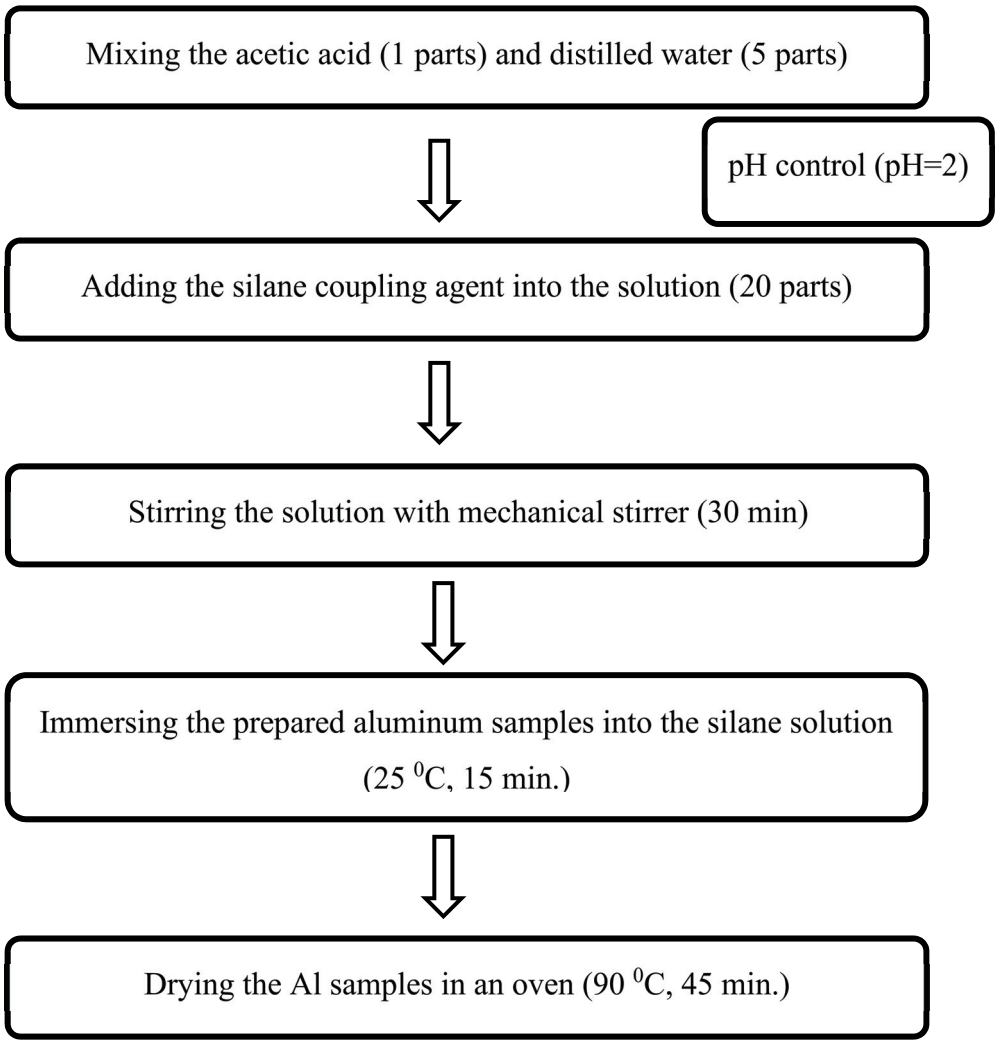

Figure 3.7. Silane treatment process for the aluminum adherends

Firstly, the aluminum surfaces were fully degreased with acetone and cleaned with water to remove contaminant at room temperature and obtain the surface which has good bondability. Then the aluminum samples were dried in oven at 100°C for 15 minutes. Finally, aluminum samples were ready for surface treatment with silane after waiting one day in ambient air.

With the aim of prepare Z-6032 silane solution, firstly acetic acid solution was prepared with a ratio of 1 parts glacial acetic acid to 5 parts distilled water to prepare acedic acid solution. then, they were stirred for 10 minutes. The solution pH was adjusted to 2 and 20 parts silane coupling agent was added into the acetic acid solution. They were stirred for 30 minutes with mechanical stirrer.

Al plate prepared for silane surface treatment were immersed into the silane solution and they were left for 15 minutes at room temperature, then removed from silane solution and dried for 45 minutes at 90^0C in oven.

For mechanical treatment of the aluminum surface, sandblasting treatment method was applied. In sandblasting process, aluminum surfaces are roughened with grit impact that is accelerated using air pressure. The air pressure was set 0,6 MPa and it was created by a compressor.

After sandblasting treated, surface roughness values (Ra, Rz) of specimens were measured by using surface roughness test machine. (Mitutoyo SJ-201). This test machine is shown in Fig.3.8. Sandblasting treated and non-treated surface roughness values of aluminum were measured. For both surfaces, average surface roughness values were determined by measurements taken at three surface points at random. As a result of these measurements, it has been determined how much surface roughness increases by sandblasting surface treatment on aluminum surface.

Figure 3.8. Surface roughness test machine

3.3.2. Surface Treatment of GFPP

In the study, the bonding surfaces of the GFPP samples prepared for all tests were mechanically treated with 240 silicon carbide abrasive paper. Afterwards, the

samples were kept in ultrasonic acetone bath for 1 hour to remove the contaminants on their surfaces and made ready for bonding.

3.3.3. Adhesive Bonding of GFPP and Al plates

Adhesive film (Bemis 3218) was placed between about 3 mm thick GFPP plate and 2 mm thick aluminum plate. Then temperature and pressure were applied. In the FMLs manufacturing process, the process temperature was determined as 130 ^{0}C and pressure as 1.2 MPa.

3.4. Mechanical Property Characterization of FMLs

In order to determine mechanical properties of specimens single lap shear, double cantilever beam (DCB) and three point bending tests were applied. In the study, all mechanical tests were performed according to relevant ASTM standards.

3.4.1. Single Lap Shear Test

Single lap shear test used for determining the bonding properties of adhesive for joining GFPP and Al and determining the shear strength of the joints.

In this test, specimens were prepared accordance with ASTM D5868. Specimen dimensions are shown in Fig. 3.9.

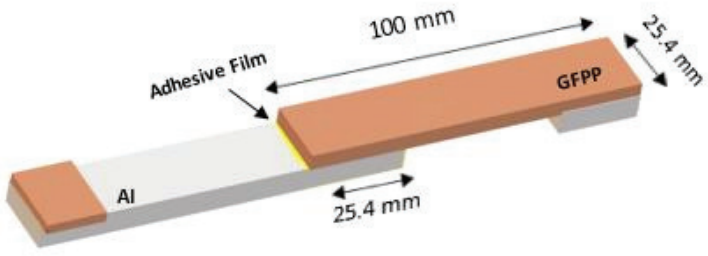

Figure 3.9. Lap shear specimen dimensions

In single lap shear test, at least 5 specimens for each different surface treatments were tested using Schimadzu™ test machine at a crosshead speed of 2 mm/min and test set up is shown in Fig.3.10.

Figure 3.10. Single lap shear test specimen during test

After single lap shear strength test, in order to determine the types of failure (adhesive, cohesive or mixed adhesive-cohesive) the adhesion surfaces of the specimens which were exposed to lap shear test were examined.

3.4.2. Double Cantilever Beam (DCB) Test

The Mode-I interlaminar fracture toughness (G_{Ic}) of the specimens was calculated by double cantilever beam (DCB) test. DCB test applied to specimens according to ASTM D5528-13. The dimensions of DCB test specimens are shown schematically in Figure 3.11.

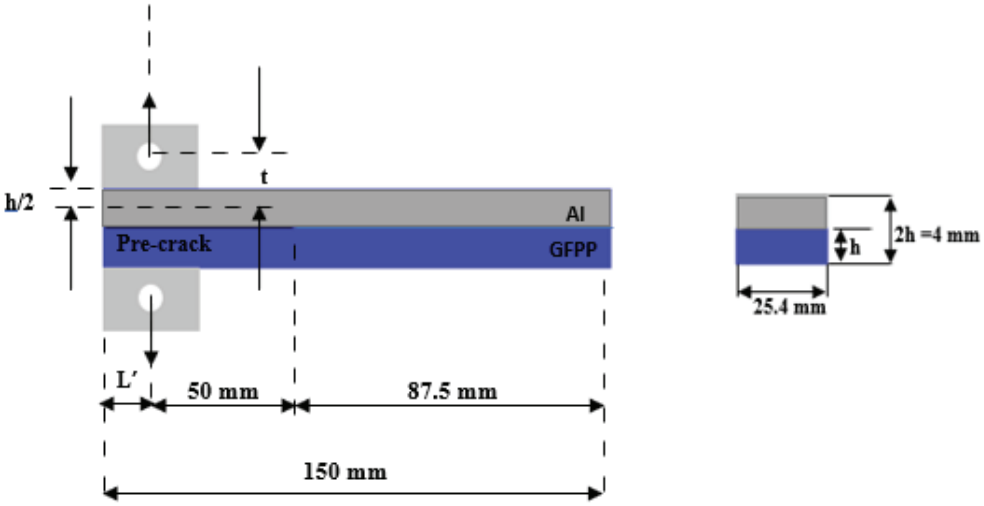

Figure 3.11. DCB specimen dimensions

The specimens were sectioned using diamond saw with 25.4 mm in width and 150 mm in length for each surface treatment techniques. The initial delamination length, a_0, was about 50 mm.

The DCB test is performed to specimens as follows; firstly, specimens were loaded and crosshead speed is set to 1 mm/min. The crack was permitted to propagate about 5mm. Then the specimens were unloaded. Finally, the specimen was reloaded until the crack propagated about 70 mm from where the crack begins. Figure 3.12 shows a DCB specimen under Mode-I loading. In order to calculate mode I interlaminar fracture toughness (G_{Ic}) values of specimens load, displacement, and crack length were recorded during the test. Also, initiation and propagation interlaminar fracture toughness values were calculated.

Figure 3.12. DCB test specimen during test

In this study, the G_{Ic} was calculated using the modified beam theory (MBT) data-reduction method, as follows:

$$G_I = \frac{F}{N}\frac{3P\delta}{2b(a+|\Delta|)} \tag{3.4}$$

where G_I is the Mode-I interlaminar fracture toughness, F and N are the correction parameters. These correction parameters can be calculated using Eq.(3.5) and

Eq(3.6) , P is the load, δ is the load point displacement, b is the specimen width, a is the delamination (crack) length, Δ is determined experimentally by generating a least squares plot of the cube root of compliance ($C^{1/3}$) as a function of delamination length. The compliance, C, is the ratio of load point displacement to the applied load and

$$F = 1 - \frac{3}{10}\left(\frac{\delta}{a}\right)^2 - \frac{3}{2}\left(\frac{\delta t}{a^2}\right) \tag{3.5}$$

$$N = 1 - \left(\frac{L'}{a}\right)^3 - \frac{9}{8}\left[1 - \left(\frac{L'}{a}\right)^2\right]\left(\frac{\delta t}{a^2}\right) - \frac{9}{35}\left(\frac{\delta}{a}\right)^2 \tag{3.6}$$

t and L' in the equations are shown in Figure 3.11.

3.4.3 Three Point Bending Test

The flexural properties of the surface treated, and reference specimens were determined from three point bending tests. Three point bending test set up is shown in Figure 3.13.

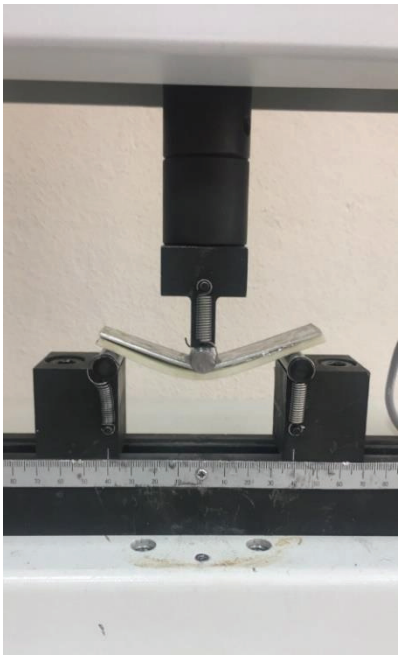

Figure 3.13. Flexural test specimen during test

Three point bending test was performed based on ASTM D790 test standard. At least, 5 specimens for each surface treatment were tested using Schimadzu™ universal test machine. This test machine crosshead speed is adjusted 2 mm/min and specimens

were sectioned using diamond saw with 20 mm in width, 5 mm in height and 100 mm in length. Length of specimens was related to span ratio, and span to thickness ratio was adjusted as 16.

Flexural stress, strain and modulus values were calculated based on equations (3.1), (3.2), and (3.3). Load and deflection values in the equations were obtained during the test.

3.5. Microstructural Characterization

In order to perform microstructural characterization of fracture surfaces of specimens Phillips™ Scanning Electron Microscope (SEM) was used. For obtaining a conductive surface, all GFPP specimens were plating with a very thin layer of gold before the SEM examinations.

The cross-sections of each laminated structures prepared by different surface pretreatment methods was taken and examined by Nikon™ optical microscope before the mechanical test. The surfaces of the samples to be examined under the optical microscope were cleaned and polished to get clear images. Prior to mechanical tests, optical microscope examination was performed to determine if the adhesion was fully functioning in samples treated with different surface treatments.

CHAPTER 4

RESULTS AND DISCUSSION

In this chapter, firstly mechanical and thermal properties of GFPP composite plate, then mechanical and microstructural properties of adhesive bonded GFPP and Al fiber metal laminates with different surface treatments are presented.

4.1 Mechanical Properties Test Results of GFPP Composite Plate

4.1.1. Tensile Test

In order to examine the tensile characteristics of noncrimp glass fiber polypropylene thermoplastic composites, manufactured at 200 ^{0}C temperature and 0.7 MPa compression pressure, tensile tests were performed according to ASTM D3039 the tensile stress-strain behavior of GFPP is showed in Fig. 4.1.

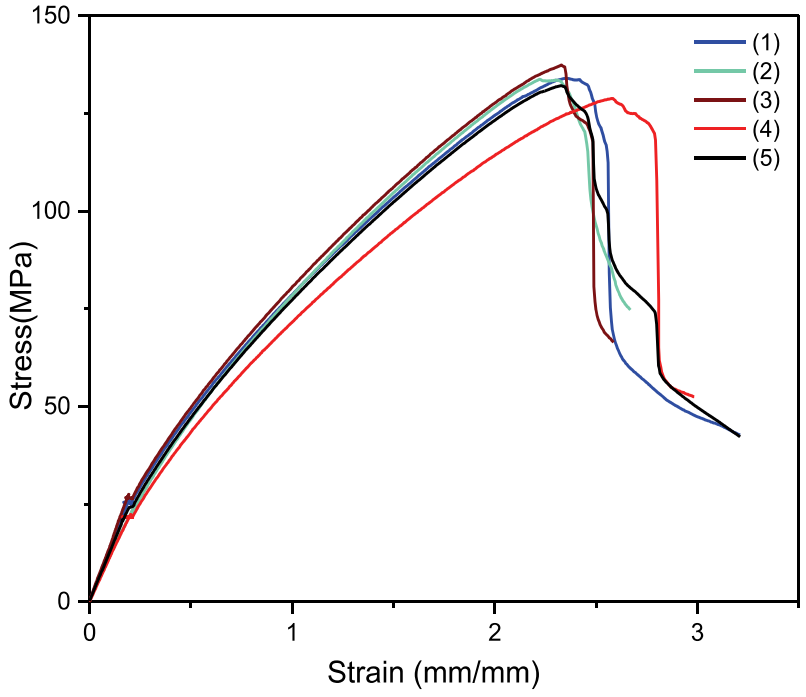

Figure 4.1. Stress vs. strain values of the composites obtained during the tensile test

Tensile strength, tensile strain and tensile modulus values are given Table 4.1. These values calculated from force-stroke data and cross-sectional area of the test specimens.

Table 4.1. Tensile properties of glass fiber/PP thermoplastic composites

Sample No	Tensile Strength (MPa)	Tensile Modulus (GPa)	Tensile Strain (MPa)
1	133.62	6.8	2.36
2	133.61	7.33	2.29
3	137.43	6.78	2.32
4	126.33	6.60	2.29
5	128.88	7.50	2.57
Average	131.97	7.01	2.37
Standard Deviation	3.91	0.35	0.11

4.1.2. Three Point Bending

Figure 4.2 indicated that the flexural stress-flexural strain behavior of GFPP composites manufactured at 200 ^{0}C temperature.

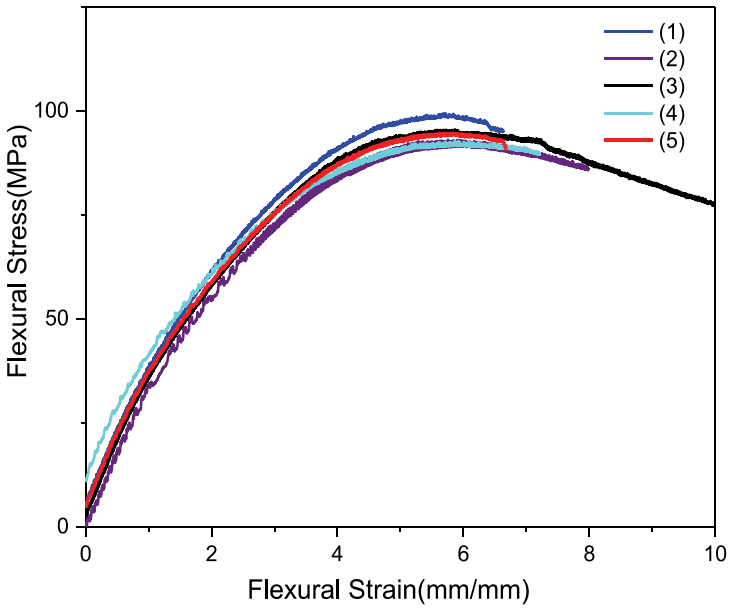

Figure 4.2. Flexural stress vs. flexural strain values of the composites obtained during the bending test

Flexural stress, flexural strain and flexural modulus values were calculated from force-stroke data and these values are illustrated in Table 4.2.

Table 4.2. Flexural properties of glass fiber/PP thermoplastic composites

Sample No	Flexural Stress (MPa)	Flexural Modulus (GPa)	Flexural Strain (MPa)
1	93.02	9.73	5.9
2	95.47	9.37	5.86
3	91.7	10.1	5.28
4	92.71	9.82	5.85
5	99.38	11.47	5.71
Average	94.46	10.10	5.72
Standard Deviation	2.52	0.73	0.23

4.1.3. Charpy Impact Test Result

Impact characteristics of the GFPP composite specimens were determined with charpy impact tests. Maximum, minimum and average absorbed energies (kJ/m^2) of the composite specimens are shown in Table 4.3. The charpy test specimens are shown in Fig. 4.3. before and after the test.

Table 4.3. Charpy impact test results

Max. Absorbed Energy (kJ/m^2)	184.28
Min.Absorbed Energy (kJ/m^2)	157.31
Avg.Absorbed Energy(kJ/m^2)	167.05
Standard Deviation	8.71

Based on the results in Table 4.3., average absorbed energy (kJ/m^2) is 167.05 kJ/m^2. These results are consistent with the other studies in the literature. Santulli et al. (2003) studied impact properties of commingled E-glass/PP composites. They reported the Charpy impact test results of glass fiber reinforced polypropylene composites. According to these test results, average absorbed energy value was calculated as about 190 kJ/m^2 (± 24.9 kJ/m^2).

Merter, et al. (2016) studied on mechanical properties of continuous glass fiber-reinforced polypropylene composites. They compared the mechanical properties of GFPP composites produced by different hybrid yarn preparation techniques. According to the Charpy impact test results, the average absorbed energy values of these composites produced with different preparation techniques vary between 115 kJ/m^2 and 198 kJ/m^2.

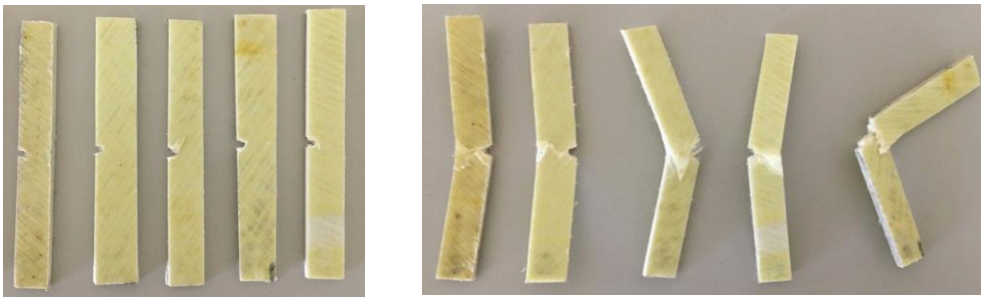

Figure 4.3. Charpy impact test samples (a) before testing, (b) after testing

4.2. Thermal Property Test Results of GFPP Composite Plate

4.2.1. Differential Scanning Calorimetry (DSC) Analysis

In order to investigate the melting temperature of glass fiber polypropylene composites DSC analyzes were performed to specimen. Figure 4.4 shows heat flow (W/g) versus temperature (^{0}C) graph of polypropylene matrix.

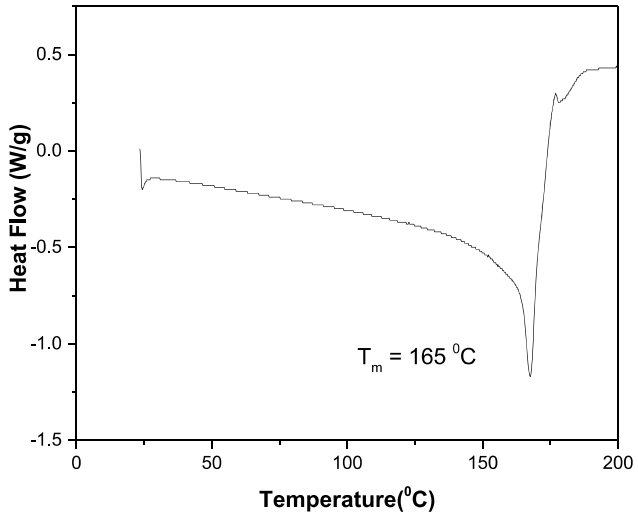

Figure 4.4. Heat flow (W/g) versus temperature (^{0}C) graph of polypropylene matrix

According to Fig.4.4, melting temperature of glass fiber/PP hybrid composite is 165 ^{0}C.

4.3. Surface Roughness Characterization of Aluminum Treated with Sandblasting

The average surface roughness values of the sandblasting treated and non-treated aluminum surface are tabulated in Table 4.4.

Table 4.4. Surface roughness parameters of sandblasting and non-treated Al specimens

Surface Roughness Values	Non-treated Al	Sandblasting Treated Al
Ra* (µm)	0.26	3.59
Rz* (µm)	1.9	23.04
* Ra = Arithmetical mean height deviation * Rz= Maximum height		

According to these results, with the sandblasting surface treatment, surface roughness parameters of aluminum (Ra and Rz) significantly increased. The sandblasted Al surface can increase the joining strength due to the improved mechanical interlocking effect.

4.4. Mechanical Properties of Al/GFPP Interfaces

4.4.1. Interfacial Single Lap Shear Strength Test Results

Interfacial properties of FML specimens were investigated with interfacial lap shear strength test and for silane treated, non-treated and sandblasting treated specimens stress-displacement curves were given in Fig 4.5, Fig 4.6, and Fig 4.7, respectively.

Figure 4.5. shows the stress-strain curves of chemically treated specimens with silane. According to results max stress is 2.06 MPa for silane treated specimens and average stress is 1.96 MPa.

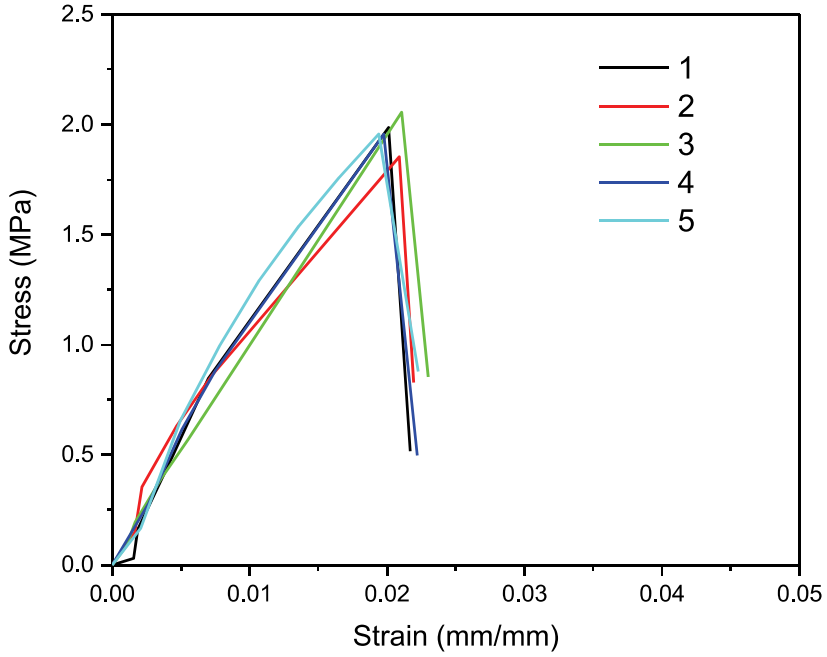

Figure 4.5. Stress vs. strain values of the silane treated FMLs obtained during the single lap shear test

Lap shear stress-strain curves of non-treated FMLs specimens are illustrated in Fig.4.6. Based on test results, maximum shear stress value is 1.79 MPa, average shear stress is obtained 1.71 MPa. As seen in Figure 4.6, for all of the specimens, stress increases linearly and reaches to maximum level at about 0.2 mm strain. In the linear region the response is elastic, and failure occurs at the maximum stress level.

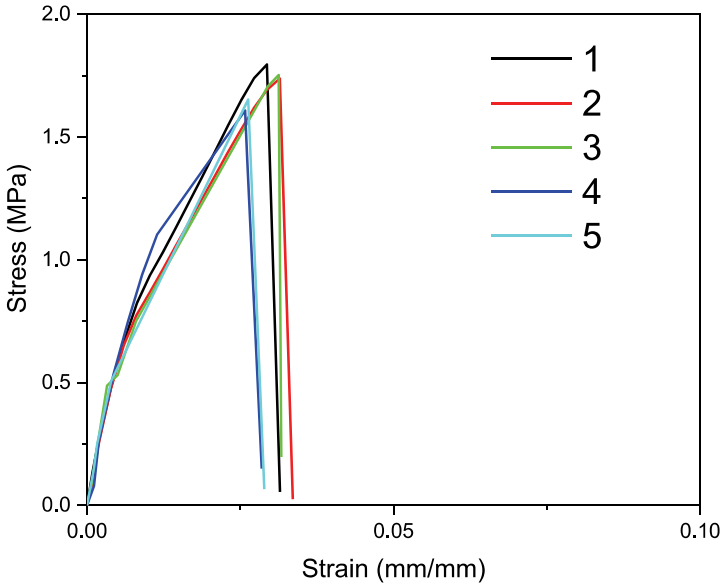

Figure 4.6. Stress vs. strain values of the non-treated FMLs obtained during the single lap shear test

Figure 4.7. shows lap shear stress-strain curve of sandlasting treated Al/GFPP specimens. According to results, maximum lap shear stress value is 2.33 MPa average shear stress is 2.15 MPa.

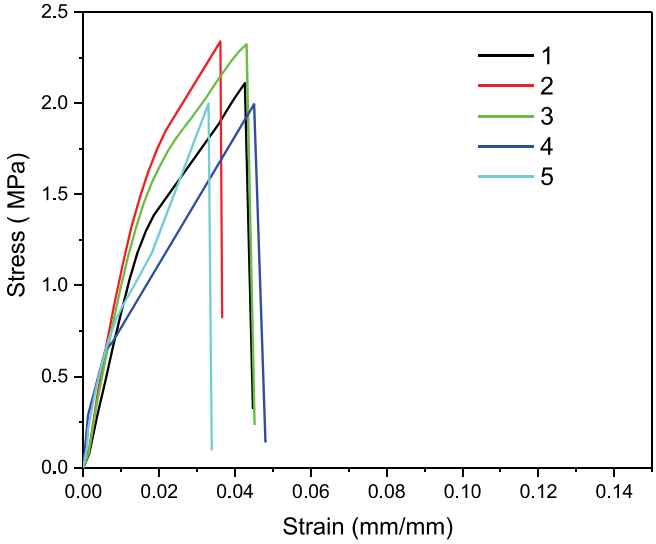

Figure 4.7. Stress vs. strain values of the sandblasting treated FMLs obtained during the single lap shear test

As seen lap shear stress-displacement figures shear stress values for all samples of Al/GFPP increased with increasing displacements until failure point then sudden drops were observed. Table 4.5 shows shear strength values were calculated from the maximum shear stresses and dimensions of the specimens.

Table 4. 5. Shear strength values of specimens

Al/GFPP Sample No	**Shear Strength (MPa)**		
	Non-treated (Reference)	**Silane Treated**	**Sandblasting Treated**
1	1.46	2.48	2.07
2	1.44	1.96	1.86
3	1.78	1.96	2.10
4	1.77	1.95	2.02
5	1.38	2.03	2.32
Average	1.61	2.08	2.08
Standard Deviation(±)	0.17	0.20	0.15

As given Table 4.5, non-treated Al/GFPP specimens have minimum shear strength values between Al and GFPP. According to Table 4.5, shear strength value of 2.08 MPa is obtained by sandblasting treatment and silane treatment of Al surfaces. A

significant improvement was achieved in the interfacial shear stresses of the samples treated with amino-based silane and sandblasting. The reason for the increase in surface treatment with silane, the chemical bonding between the amino group of the Z-6032 silane and the polypropylene as expected (Demjén, et al. 1999).

The reason for the increase in the strength of the surface treated by sandblasting is the increase in the roughness values of the aluminum surface by means of sandblasting, increasing the surface area of adhesion and ensuring that the adhesive film penetrates the surface better.

4.4.2. Mode-I Fracture Toughness Test Results of GFPP/Al Hybrid Structures

The mode-I fracture tougness values (G_{Ic}) were calculated for silane treated, non-treated and sandblasting treated specimens using Eq. 3.4 of modified beam theory (MBT) and shown in figures 4.8, 4.9, 4.10 respectively.

The maximum G_{Ic} value of silane treated specimens was determined as 0.28 kJ/m^2. The initiation and propagation G_{Ic} values for the silane treated specimens were calculated 0.04 and 0.13 kJ/m^2 respectively.

According to the Figure 4.8, the G_{Ic} values show a tendency to increase with increasing delamination length. This is due to the chemical bonding occurs between the silane and the GFPP on the adhesion surface and thus resulting glass fiber bridging effect.

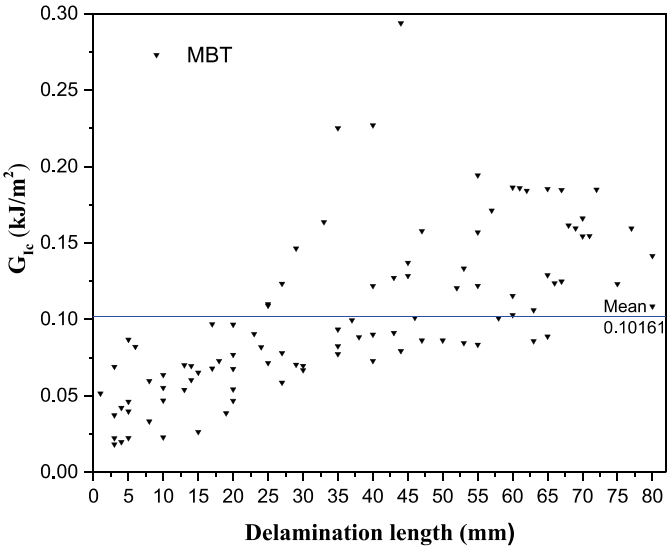

Figure 4.8. The mode-I fracture toughness values (G_{Ic}) of silane treated specimens

Figure 4.9 shows G_{Ic}-delamination length graph of non-treated samples. As seen in Figure 4.9 maximum G_{Ic} value is 0.13 kJ/m^2 , average G_{Ic} value is about 0.05 kJ/m^2. The initiation and propagation G_{Ic} values for non-treated specimens were calculated as 0.04 and 0.05 kJ/m^2 respectively. For non-treated samples, there was no tendency to increase in G_{Ic} values as the length of delamination increased.

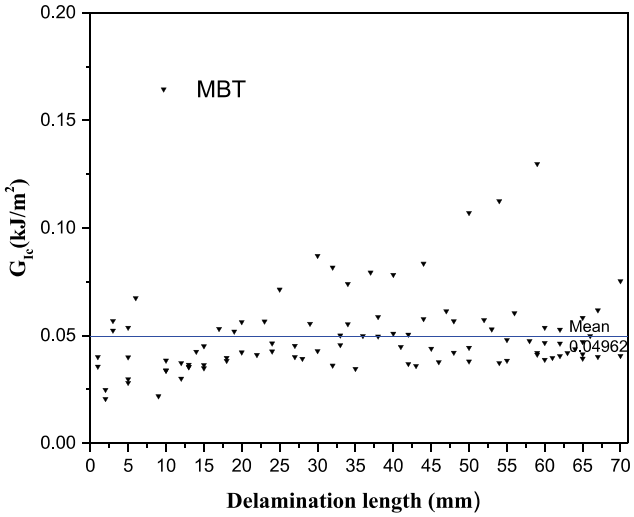

Figure 4.9. The mode-I fracture toughness values (G_{Ic}) of non -treated specimens

Figure 4.10 shows G_{Ic} data vs delamination length graphs of sandblasting treated specimens. The maximum G_{Ic} value is 0.08 kJ/m^2, average G_{Ic} value is about 0.04 kJ/m^2. From the data taken during the test the initiation and propagation G_{Ic} values for sandblasting treated specimens were calculated 0.03 and 0.04 kJ/m^2 respectively.

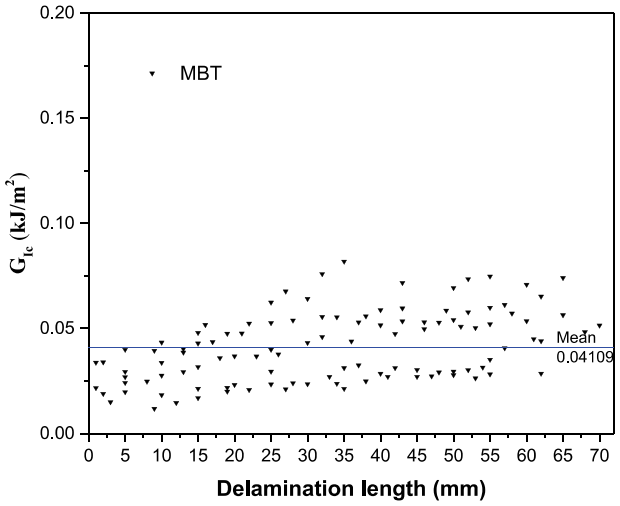

Figure 4.10. The mode-I fracture toughness values (GIc) of sandblasting treated specimens

As seen in Figure 4.10 sandblasting treated specimens have more stable crack propagation than reference specimens and specimens treated with other technique.

In order to evaluate the effect of chemical etching and sandblasting surface treatments on the adhesion surface, Shimamoto, et al. (2016) have performed the DCB test to GFPP/Al samples bonded with the welded joint. They investigated specimens with the chemical etching surface treatment have approximately four times larger critical energy release rates than sandblasted specimens. In this study, they showed that the average critical energy release rate of silane treated specimens was about 0.050 kJ/m^2. The AMALPHA treatment was chosen as the chemical etching method and average critical energy release rate of these specimens was 0.23 kJ/m^2. Also, they indicated that the critical energy release rates do not depend on the chemical etching depth.

In order to compare DCB test results of each specimens easily, the G_{Ic}-delamination length (a) values of silane treated, sandblasting treated and non-treated specimens are given in Figure 4.11. These results indicated that the G_{Ic} values of silane-treated specimens are approximately 2.5 times larger than others. G_{Ic} values of non-treated and sand blasting-treated specimens were observed to be very close to each other.

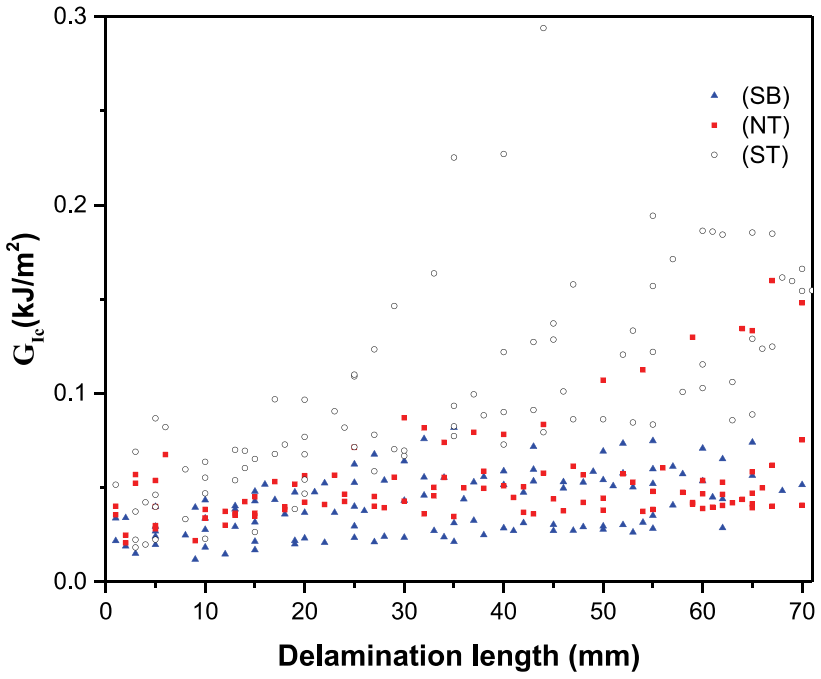

Figure 4.11. G_{Ic} vs. delamination length (a) values of silane treated, sandblasting treated and non-treated specimens

4.4.3. Flexural Properties Test Results of GFPP/Al Hybrid Structures

Load- displacement curves of silane treated, non-treated and sandblasting treated specimens are given in Fig 4.12, Fig. 4.13, and Fig.4.14 respectively.

As seen in Fig. 4.12, the specimens treated with silane the first failure observed on about 1 mm (there is a sudden drop in load values). However, with increasing displacement values, the samples can carry higher load values than the load values they carry up to the first failure. The maximum load value is reached when the displacement value is about 10 mm.

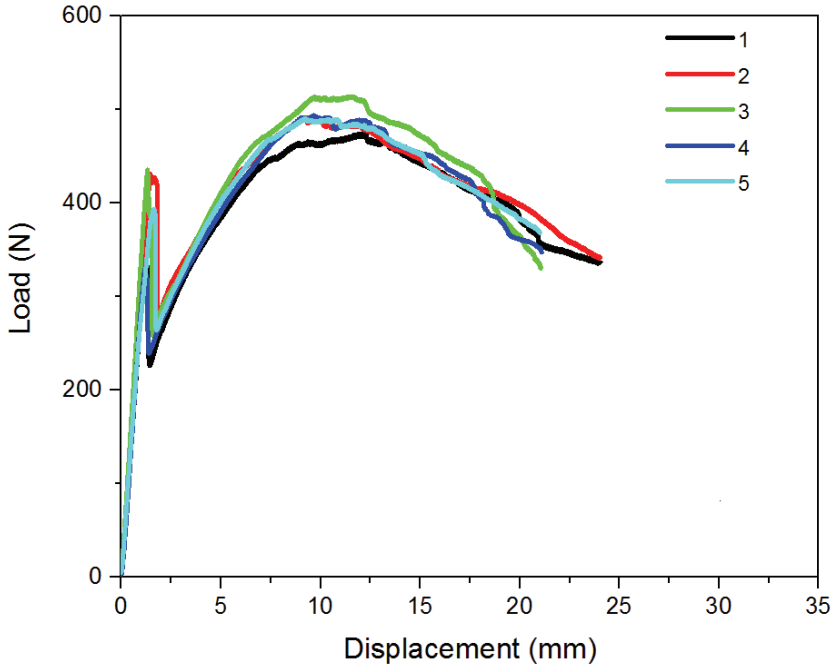

Figure 4.12. Load vs displacement curves of the silane treated specimens obtained during the bending test

Ultimate bending load, bending stiffness and displacement at failure values of silane treated specimens are given in Table 4.6. According to this table, average ultimate bending load was found about 500 N, bending stiffness was 298 N/mm average displacement at failure was calculated as 10.52 mm. According to these results, in silane-treated samples, although the sample received the first failure at approximately 1 mm displacement value, it continued to carry load and the displacement values at the failure were found to be about 10 mm.

Table 4.6. Flexural properties of silane treated specimens

Sample No	Ultimate Bending Load (N)	Bending Stiffness (N/mm)	Displacement at Failure (mm)
1	496.95	288.9	12.3
2	501.23	310.8	9.91
3	513.75	340.64	11.49
4	499.55	298.41	9.66
5	490.4	250.9	9.22
Average	500.38	297.93	10.52
Standard Deviation	8.54	29.27	1.18

In non-treated specimens results, there is a sudden drop in load values after reaching a maximum certain load value in non-treated samples. At these displacement values (about 2 mm), the samples were failured first and there was a slight increase in the load values after sudden drop. However, these load values were not as high as the load values before the first failure.

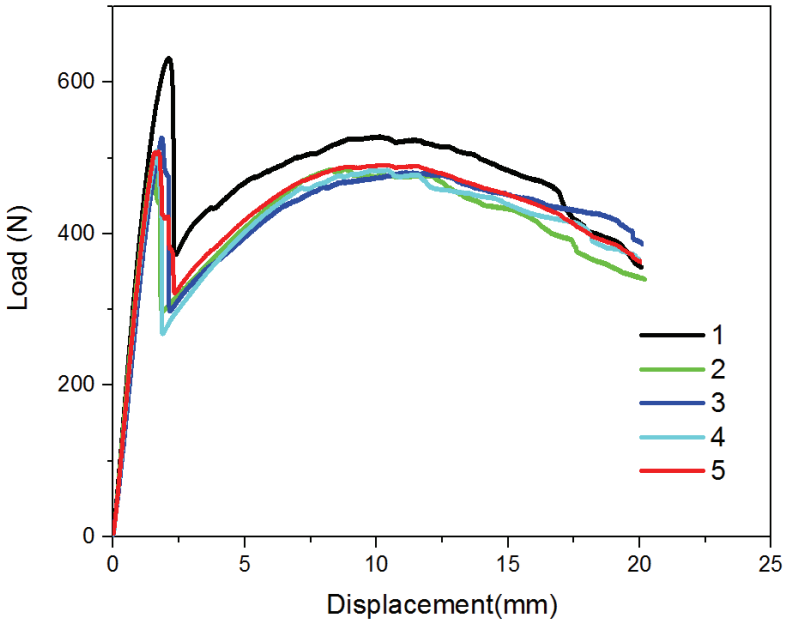

Figure 4.13. Load vs. displacement curves of the non-treated specimens obtained during the bending test

Ultimate bending load, bending stiffness and displacement at failure values of non-treated specimens are given in Table 4.7. As shown in Table 4.7 average ultimate bending load was found as 518 N

Table 4.7. Flexural properties of non-treated specimens

Sample No	Ultimate Bending Load (N)	Bending Stiffness (N/mm)	Displacement at Failure (mm)
1	615.25	314.41	2.1
2	490.85	288.52	10.24
3	496.25	342.38	1.54
4	493.83	301.98	1.83
5	495.5	323.55	1.66
Average	518.34	314.17	3.47
Standard Deviation	48.50	18.39	3.39

According to flexural test results of the sand-blasting treated specimens (Figure 4.14), load values increased up to a certain point with increasing displacement and then showed a sudden drop. The displacement value of the sudden drop is the point where the sample was first failure. Load values increased after a sudden drop and the maximum value of load is very close to the maximum load value at the point of the first failure.

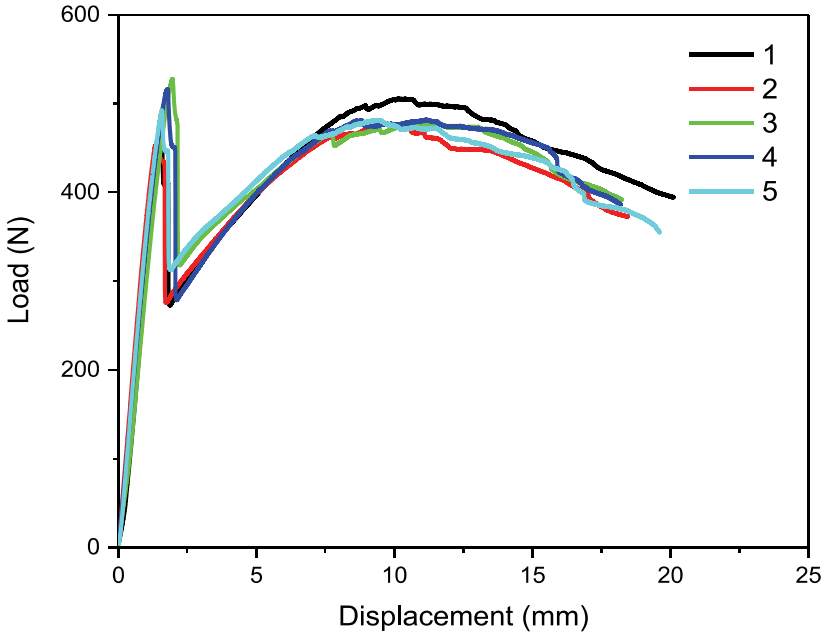

Figure 4.14. Load vs. displacement curves of the sandblasting treated specimens obtained during the bending test

As shown in Table 4.8, ultimate bending load, bending stiffness and displacement at failure values of sand blasting treated specimens are 504 N, 313 N/mm, 7.04 mm respectively.

Table 4.8. Flexural properties of sandblasting treated specimens

Sample No	Ultimate Bending Load (N)	Bending Stiffness (N/mm)	Displacement at Failure (mm)
1	505.85	306.11	10.14
2	477.66	326.09	9.73
3	527.93	296.9	1.96
4	516.52	305.2	11.77
5	492.15	332.3	1.58
Average	504.02	313.32	7.04
Standard Deviation	17.70	13.50	4.35

According to the ultimate bending load values of the silane treated (ST), non-treated (NT) and treated with sandblasting (SB) specimens. the ultimate bending load values are very close to each other. As seen in the flexural test results, treat operations on the adhesion surface did not change the bending load values very much, but it allowed the sample to continue to carry the load after first failure and even more than the stress it carried up to the first failure.

4.5. Characterization of Failure in Adhesively Bonded Surface of Single Lap Shear Test Specimens

The types of failure (adhesive, cohesive or mixed adhesive-cohesive) of the single lap shear applied specimens were determined by examining the adhesion surfaces.

Figure 4.15 (a) shows the adhesion surface of non-treated specimens. As seen in Fig. 4.16, it was observed that the adhesive remained on the surface of only one of the adherends (only Al surface). On the surface of the GFPP no residues of adhesive were found. This means that the type of failure seen in non-treated specimens is adhesive failure along adhesive-adherend interface.

The adhesion surface of silane treated specimens is shown in Figure 4.15 (b). According to this figure a portion of the adhesive was found on the surface of Al, the other part remained on the surface of GFPP. This type of failure is interpreted as a mixed mode (adhesive and cohesive), mostly cohesive failure type.

Figure 4.15 (c) shows the adhesion surface of sandblasting treated specimens. In this figure it has been observed that the residues of adhesive are on both surfaces, or even on the adhesive of the Al surface, the residues of GFPP plate. Therefore, cohesive failure was observed in sandblasting treated specimens.

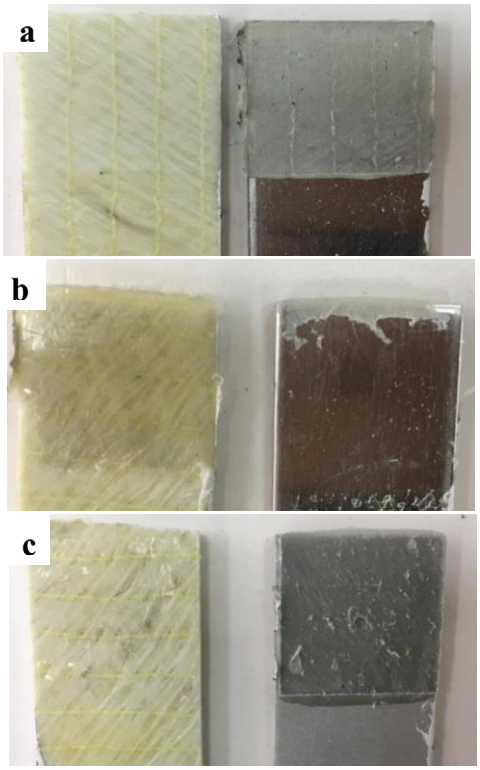

Figure 4.15. Fracture surface of (a) non-treated, (b) silane treated,(c) sandblasting treated specimens after single lap shear test

4.6. Microstructural Characterization Results of Al/GFPP Hybrid Structures

The optical microscope was used to perform the microstructural examination of the adhesively bonded laminates cross sections. Figure 4.16 shows the images of sandblasting treated, non-treated, and silane treated specimens microstructural characterization by optical microscope, respectively. According to these micrographs in all samples treated with different surface treatments, continuous bonding was provided on the adhesion surface of the between GFPP and Al and no unbound or defective regions were observed.

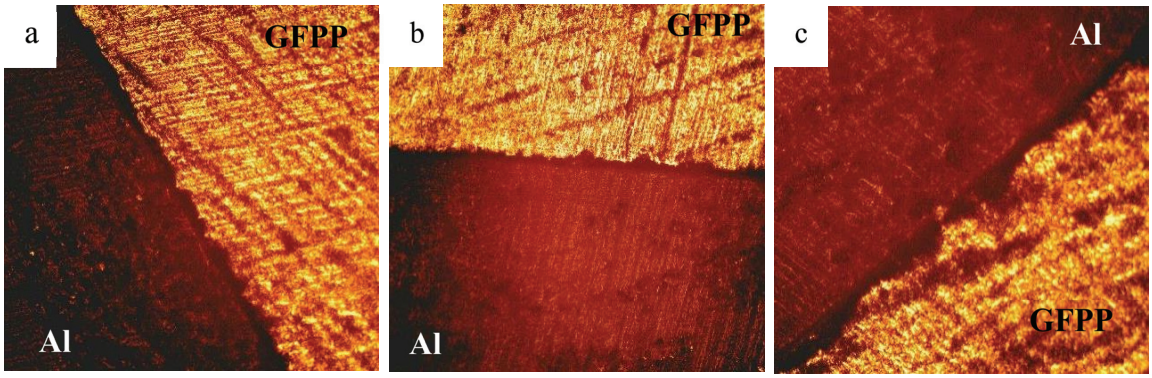

Figure 4.16. Optical images of cross sections of GFPP/Al specimens a) sandblasting treated structures (b) non-treated (c)silane treated structures (20x)

Aim to characterization of the failure modes of FMLs specimens after single lap shear testing SEM was used.

SEM micrographs of fracture surface of the Al side of fiber metal laminated with silane treated, sandblasting treated, and non-treated specimens were illustrated in Figure 4.17 respectively.

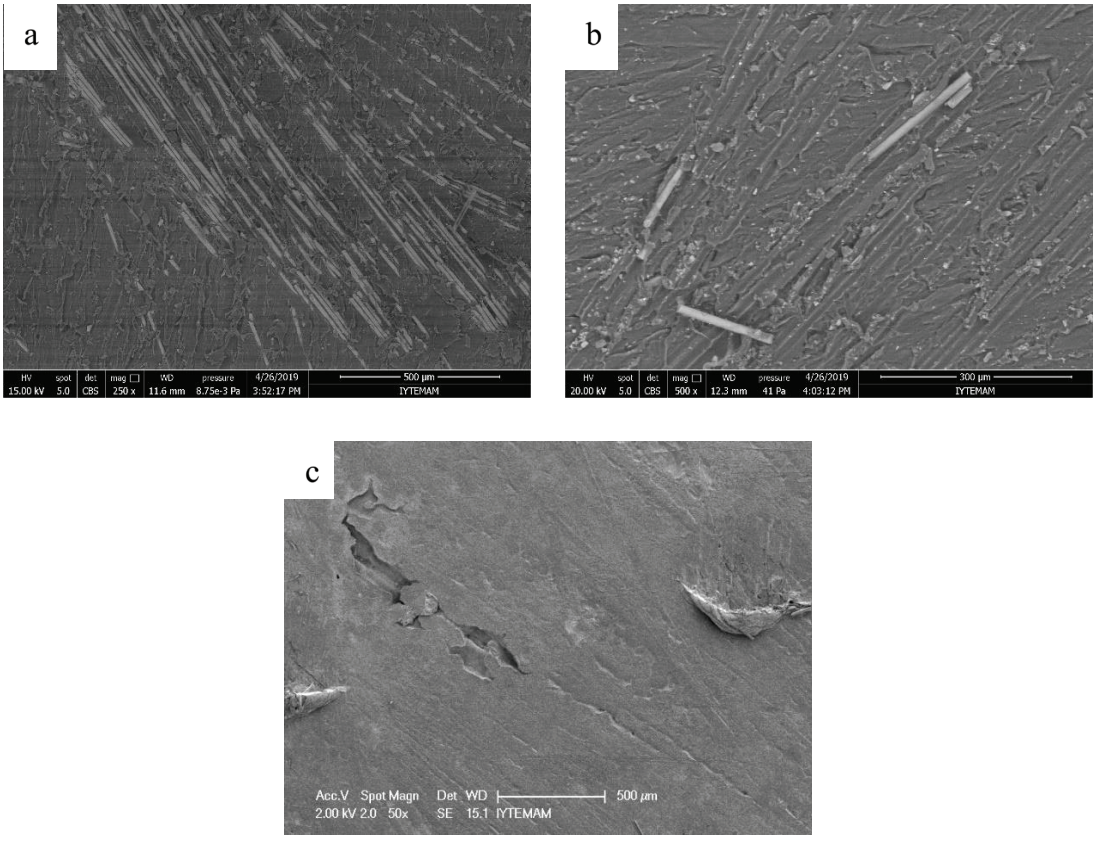

Figure 4.17. Fracture surface SEM images Al adherends of Al / GFPP with (a)silane treated (b)sandblasting treated (c)non-treated structures

According to the SEM images, residues from the GFPP plate were observed on the silane and sandblasting treated Al bonded surfaces, while no residues were observed from the GFPP plate on the non-treated Al adhesively bonded surface. GFPP residues on the non-treated Al surface are not observed because there is no chemical and physical interaction at the bonded interface and adhesive failure is observed in these samples. The glass fiber and matrix material presence in the silane and sandblasting treated Al samples is the proof that the failure type seen in these samples is a cohesive failure. This shows that adhesion at the GFPP / Al interface is better than non-treated samples.

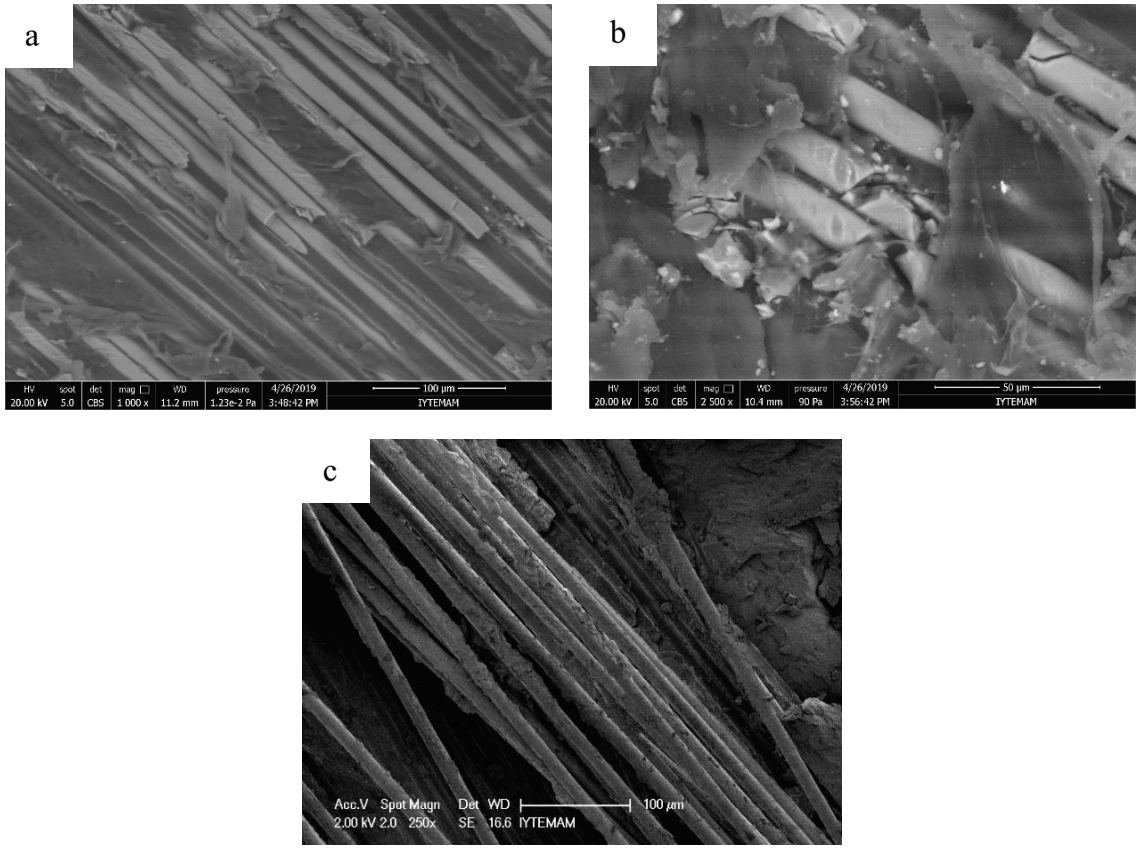

Figure 4.18. Fracture surface SEM images GFPP adherends of Al / GFPP with (a)silane treated (b)sandblasting treated (c)non-treated structures

Fig. 4.18 shows the images for silane treated, sandblasting treated and non-treated of GFPP fracture interface at higher magnification respectively. Also, they indicate that deformation around fibers occurs for treated specimens. It is seen that the deformation of the polypropylene matrix and break and pull out of fibers are very common for treated specimens. (Fig. 4.18 (a) and (b)). It proves that the failure is

cohesive through the polypropylene composite plate. These deformations in the fiber and matrix indicate that plastic deformation occurs in the GFPP specimens during the lap shear test. This is an evidence of the good adhesively bonded of the treated specimens to each other. However, no deformation was observed to the matrix and the fibers in non-treated specimens. This again indicates that the adhesive failure occurred along the adhesive-adherend interface for these specimens.

CHAPTER 5

CONCLUSIONS

In this study, initially glass fiber reinforced polypropylene matrix composites were successfully manufactured from hybrid fabrics by hot press compression process. Manufactured thermoplastic composite plates were characterized by some mechanical tests. Then, to produce fiber metal laminated structures using the adhesive film the produced GFPP plate and Al were used as the adherends. While manufacturing FMLs, various surface modification technique were applied for the good adhesion of GFPP and Al interface and their effect on the adhesive properties of GFPP/Al laminates were reported. Surface modification techniques applied to aluminum bonded surface are silane treatment and sandblasting treatment. After sandblasting surface treatment, surface roughness parameters (Ra and Rz) of aluminum was determined by using surface roughness test machine. According to the results of the measurements on the surface of Al samples treated with sandblasting and not treated, those parameters (Ra and Rz) significantly increased with the sandblasting surface treatment.

Tensile properties, flexural properties, impact energy properties and melting temperature of GFPP composite were determined within the study to characterize the GFPP composite plate.

Tensile test was performed so as to investigate tensile properties of the GFPP composite plate. The tensile strength value was obtained 132 MPa and elastic modulus 7 GPa.

Flexural test was applied for the purpose of investigating the flexural properties of the GFPP composite specimens. Flexural strength value was calculated as 94.46 MPa. Flexural modulus was found as 10.10 GPa.

The glass fiber polypropylene composite plate impact properties were investigated with Charpy (V-notch) impact test and absorbed energy values were evaluated from the taken data. According to test results, average absorbed energy value was obtained 167.05 kJ/m^2. The absorbed energy values vary between 157.31 and 184.28 kJ/m^2. These results are compatible with the other studies in literature.

Single lap-shear, DCB and flexural tests were applied to show the effects of different surface pre-treatment techniques on adhesive characteristics of GFPP/Al structures.

Single lap shear test was performed to silane treated, sandblasting treated and non-treated specimens (non-treated specimens were taken as reference for all tests). Based on test results, the shear strength values of the silane treated and sandblasting treated specimens were very close to each other. (2.08 MPa) The shear strength values of the GFPP/Al adhesion surfaces increased by 30% compared to the reference specimen via surface pre-treatment techniques. The reason for the increase in the shear strength values of the silane treated specimens is formation of a chemical bond between the amino group of the Z-6032 silane and PP. The reason of the increase in the shear strength of the sandblasting treated specimens is the increase in the surface area of bonded, the increase of the surface roughness and thus the better penetration of the adhesive to adherends.

The Mode-I interlaminar fracture toughness of the samples was determined by double cantilever beam (DCB) test. From the results the G_{Ic} values of silane-treated specimens are approximately 2.5 times larger than others. G_{Ic} values of non-treated and sand blasting-treated specimens were observed to be very close to each other. It can be interpreted that sandblasting treated specimens have more stable crack propagation than reference specimens and specimens treated silane.

The flexural properties of GFPP/Al specimens were determined with three point bending test. Ultimate bending load values of silane treated, non-treated and sabdlasting treated specimens are 500,518, and 504 N respectively. No significant change was observed in the ultimate bending load values of the treated specimens compared to the reference sample. As seen in the flexural test results, treat operations on the adhesion surface did not cause dramatical change on ultimate bending load values, but it allowed the sample to continue carrying the load after first failure (there is a sudden drop in stress values) and even reach more than the max stress it carried until the first failure.

According to optical microscope images, continuous bonding was provided on the interface of the GFPP and Al and no unbound or defective regions were observed for each specimens manufactured with different surface treatment techniques.

In order to characterization of failure in adhesively bonded surface, fracture surfaces of the specimens that lap shear test performed were examined. As a result of the examinations, adhesive failure along adhesive-adherend interface is seen in only

non-treated specimens. Cohesive failure type was observed in silane and sandblasting surface treated specimens.

According to the SEM images for fractured surfaces of silane and sanblasting treated GFPP/Al demonstrated better adhesion characteristics owing to the polypropylene layer observed on the fractured surface of Al. SEM images for fractured surface of GFPP, in silane and sandblasting treated specimens, it was observed that there were damages on the fibers in the matrix. The data would seem to suggest that the failure type during the lap shear test is cohesive failure in these specimens. In the non-treated specimens, no damage was observed to the fibers.

REFERENCES

Abdullah, M. R., Y. Prawoto, and W. J. Cantwell. 2015. "Interfacial Fracture of the Fibre-Metal Laminates Based on Fibre Reinforced Thermoplastics." *Materials and Design* 66 (PB). Elsevier Ltd: 446–52. doi:10.1016/j.matdes.2014.03.058.

Astigarraga, Victoria, Koldo Gondra, Ángel Valea, and Goizane Pardo Aurrekoetxea. 2019. "Improvement of Adhesive Bonding of Polypropylene and Maleic Anhydride Grafted Polypropylene Blends to Aluminium by Means of Addition of Cyclic Butylene Terephthalate." *Journal of Adhesion* 95 (4). Taylor & Francis: 286–307. doi:10.1080/00218464.2018.1437415.

ASTM-American Society for Testing and Materials. 2001. "ASTM Standard D5528: Test Method for Mode I Interlaminar Fracture Toughness of Unidirectional Fiber-Reinforced Polymer Matrix Composites 1." *Annual Book of ASTM Standards* 01 (Mode I): 1–12. doi:10.1520/D5528-13.2.

Berry, Douglas H., and Apinan Namkanisorn. 2005. "Fracture Toughness of a Silane Coupled Polymer-Metal Interface: Silane Concentration Effects." *Journal of Adhesion* 81 (3–4): 347–70. doi:10.1080/00218460590944657.

Broughton, W. 2012. "Testing the Mechanical, Thermal and Chemical Properties of Adhesives for Marine Environments." *Adhesives in Marine Engineering*, 99–154. doi:10.1016/B978-1-84569-452-4.50006-0.

Callister, William D, and David G Rethwisch. 2007. *Materials Science and Engineering: An Introduction*. Vol. 7. John Wiley & Sons New York.

Cantwell, W J. 2000. "The Mechanical Properties of Fibre-Metal Laminates Based on Glass Fibre Reinforced Polypropylene." *Composites Science and Technology* 60 (7). Elsevier: 1085–94.

Cerny, Jennifer, and Gregory Morscher. 2006. "Adhesive Bonding of Titanium to Carbon-Carbon Composites for Heat Rejection Systems."

Chen, Ming An, Hui Zhong Li, and Xin Ming Zhang. 2007. "Improvement of Shear Strength of Aluminium-Polypropylene Lap Joints by Grafting Maleic Anhydride onto Polypropylene." *International Journal of Adhesion and Adhesives* 27 (3): 175–87. doi:10.1016/j.ijadhadh.2006.01.008.

Correia, Sergio, Vitor Anes, and Luis Reis. 2018. “Effect of Surface Treatment on Adhesively Bonded Aluminium-Aluminium Joints Regarding Aeronautical Structures.” *Engineering Failure Analysis* 84 (November 2017). Elsevier: 34–45. doi:10.1016/j.engfailanal.2017.10.010.

Critchlow, G. W., and D. M. Brewis. 1996. “Review of Surface Pretreatments for Aluminium Alloys.” *International Journal of Adhesion and Adhesives* 16 (4): 255–75. doi:10.1016/S0143-7496(96)00014-0.

Demjén, Zoltán, Béla Pukánszky, and József Nagy. 1999. “Possible Coupling Reactions of Functional Silanes and Polypropylene.” *Polymer* 40 (7): 1763–73. doi:10.1016/S0032-3861(98)00396-6.

Dow, The, and Chemical Company. 2017. “XIAMETER ™ OFS-6032 Silane,” no. 95: 1–8.

Etcheverry, Mariana, and Silvia E. Barbosa. 2012. “Glass Fiber Reinforced Polypropylene Mechanical Properties Enhancement by Adhesion Improvement.” *Materials* 5 (6): 1084–1113. doi:10.3390/ma5061084.

Freitas, Sofia Teixeira De, and Jos Sinke. 2014. “Adhesion Properties of Bonded Composite-to-Aluminium Joints Using Peel Tests.” *Journal of Adhesion* 90 (5–6): 511–25. doi:10.1080/00218464.2013.850424.

Gadelmawla E.S., Koura M. M., Maksoud T. M. A., Elewa I. M., Soliman H.H. 2002. “Roughness Parameters” *Journal of Materials Processing Technology* 123: 133-145

Goushegir, S M. 2015. “Friction Spot Joining of Polymer-Metal Hybrid Structures.” *Welding in the World* 49 (0): 2–4. doi:http://dx.doi.org/10.1007/s40194-016-0368-y.

Green, M. D., F. J. Guild, and R. D. Adams. 2002. “Characterisation and Comparison of Industrially Pre-Treated Homopolymer Polypropylene, HF 135M.” *International Journal of Adhesion and Adhesives* 22 (1): 81–90. doi:10.1016/S0143-7496(01)00040-9.

Guild, F. J., M. D. Green, R. Stewart, and V. Goodship. 2008. “Air-Plasma Pre-Treatment for Polypropylene Automotive Bumpers.” *Journal of Adhesion* 84 (6): 530–42. doi:10.1080/00218460802161574.

Honkanen, Mari, Maija Hoikkanen, Minnamari Vippola, Jyrki Vuorinen, and Toivo Lepistö. 2009. “Metal-Plastic Adhesion in Injection-Molded Hybrids.” *Journal of Adhesion Science and Technology* 23 (13–14): 1747–61. doi:10.1163/016942409X12489445844435.

Huang, Zhequn, Sumio Sugiyama, and Jun Yanagimoto. 2014. “Applicability of Adhesive-Embossing Hybrid Joining Process to Glass-Fiber-Reinforced Plastic and Metallic Thin Sheets.” *Journal of Materials Processing Technology* 214 (10). Elsevier B.V.: 2018–28. doi:10.1016/j.jmatprotec.2013.11.020.

Kim, Jin Gyu, Sang Wook Park, Soon Ho Yoon, and Dai Gil Lee. 2010. “Optimum Silane Treatment for the Adhesively Bonded Aluminum Adherends at the Cryogenic Temperature.” *Journal of Adhesion Science and Technology* 24 (4): 775–87. doi:10.1163/016942409X12579497420843.

Kim, Won Seock, and Jung Ju Lee. 2007. “Adhesion Strength and Fatigue Life Improvement of Co-Cured Composite/Metal Lap Joints by Silane-Based Interphase Formation.” *Journal of Adhesion Science and Technology* 21 (2): 125–40. doi:10.1163/156856107780437462.

Kleffel, Tobias, and Dietmar Drummer. 2017. “Investigating the Suitability of Roughness Parameters to Assess the Bond Strength of Polymer-Metal Hybrid Structures with Mechanical Adhesion.” *Composites Part B: Engineering* 117. Elsevier Ltd: 20–25. doi:10.1016/j.compositesb.2017.02.042.

Leena, K., K. K. Athira, S. Bhuvaneswari, S. Suraj, and V. Lakshmana Rao. 2016. “Effect of Surface Pre-Treatment on Surface Characteristics and Adhesive Bond Strength of Aluminium Alloy.” *International Journal of Adhesion and Adhesives* 70. Elsevier: 265–70. doi:10.1016/j.ijadhadh.2016.07.012.

Matsuzaki, Ryosuke, Motoko Shibata, and Akira Todoroki. 2008. “Improving Performance of GFRP/Aluminum Single Lap Joints Using Bolted/Co-Cured Hybrid Method.” *Composites Part A: Applied Science and Manufacturing* 39 (2): 154–63. doi:10.1016/j.compositesa.2007.11.009.

Merter, N. Emrah, Gülnur Baüer, and Metin Tanoğlu. 2016. “Effects of Hybrid Yarn Preparation Technique and Fiber Sizing on the Mechanical Properties of Continuous Glass Fiber-Reinforced Polypropylene Composites.” *Journal of Composite Materials* 50 (12): 1697–1706. doi:10.1177/0021998315595710.

Messler, Robert W. 2004. *Joining of Materials and Structures: From Pragmatic Process to Enabling Technology*. *Joining of Materials and Structures: From Pragmatic Process to Enabling Technology*. doi:10.1016/B978-0-7506-7757-8.X5000-3.

Messler, Robert W. 2000. "Features Trends in Key Joining Technologies for the Twenty-First Century" 20 (2): 118–28.

Molitor, P., and T. Young. 2002. "Adhesives Bonding of a Titanium Alloy to a Glass Fibre Reinforced Composite Material." *International Journal of Adhesion and Adhesives* 22 (2): 101–7. doi:10.1016/S0143-7496(01)00041-0.

Ochoa-Putman, Carol, and Uday K. Vaidya. 2011. "Mechanisms of Interfacial Adhesion in Metal-Polymer Composites - Effect of Chemical Treatment." *Composites Part A: Applied Science and Manufacturing* 42 (8). Elsevier Ltd: 906–15. doi:10.1016/j.compositesa.2011.03.019.

Ostapiuk, Monika, Barbara Surowska, and Jarosław Bieniaś. 2014. "Interface Analysis of Fiber Metal Laminates." *Composite Interfaces* 21 (4). Taylor & Francis: 309–18. doi:10.1080/15685543.2014.854527.

Park, Sang Yoon, Won Jong Choi, Heung Soap Choi, Hyuk Kwon, and Sang Hwan Kim. 2010. "Recent Trends in Surface Treatment Technologies for Airframe Adhesive Bonding Processing: A Review (1995-2008)." *Journal of Adhesion* 86 (2): 192–221. doi:10.1080/00218460903418345.

Pramanik, A., A. K. Basak, Y. Dong, P. K. Sarker, M. S. Uddin, G. Littlefair, A. R. Dixit, and S. Chattopadhyaya. 2017. "Joining of Carbon Fibre Reinforced Polymer (CFRP) Composites and Aluminium Alloys – A Review." *Composites Part A: Applied Science and Manufacturing* 101. Elsevier Ltd: 1–29. doi:10.1016/j.compositesa.2017.06.007.

Rafiq, S, F Ahmad, Z Man, and S Maitra. 2011. "Silica-Polymer Nanocomposite Membranes for Gas Separation - A Review, Part 2." *InterCeram: International Ceramic Review* 60 (1): 8–13. https://www.scopus.com/inward/record.uri?eid=2-s2.0-84856136889&partnerID=40&md5=530a0402ccb61b5fc41387dab93818c1.

Reyes, G., and H. Kang. 2007. "Mechanical Behavior of Lightweight Thermoplastic Fiber-Metal Laminates." *Journal of Materials Processing Technology* 186 (1–3): 284–90. doi:10.1016/j.jmatprotec.2006.12.050.

Ribeiro, T. E.A., R. D.S.G. Campilho, L. F.M. da Silva, and L. Goglio. 2016. “Damage Analysis of Composite-Aluminium Adhesively-Bonded Single-Lap Joints.” *Composite Structures* 136. Elsevier Ltd: 25–33. doi:10.1016/j.compstruct.2015.09.054.

Rudawska, Anna. 2010. “Adhesive Joint Strength of Hybrid Assemblies: Titanium Sheet-Composites and Aluminium Sheet-CompositesExperimental and Numerical Verification.” *International Journal of Adhesion and Adhesives* 30 (7). Elsevier: 574–82. doi:10.1016/j.ijadhadh.2010.05.006.

Santulli, C., R. Brooks, A. C. Long, N. A. Warrior, and C. D. Rudd. 2003. “Impact Properties of Compression Moulded Commingled E-Glass–Polypropylene Composites.” *Plastics, Rubber and Composites* 31 (6): 270–77. doi:10.1179/146580102225004983.

Shimamoto, K., Y. Sekiguchi, and C. Sato. 2016. “Effects of Surface Treatment on the Critical Energy Release Rates of Welded Joints between Glass Fiber Reinforced Polypropylene and a Metal.” *International Journal of Adhesion and Adhesives* 67. Elsevier: 31–37. doi:10.1016/j.ijadhadh.2015.12.022.

Sinmazçelik, Tamer, Egemen Avcu, Mustafa Özgür Bora, and Onur Çoban. 2011. “A Review: Fibre Metal Laminates, Background, Bonding Types and Applied Test Methods.” *Materials and Design* 32 (7): 3671–85. doi:10.1016/j.matdes.2011.03.011.

Spaggiari, A., and E. Dragoni. 2013. “Effect of Mechanical Surface Treatment on the Static Strength of Adhesive Lap Joints.” *Journal of Adhesion* 89 (9): 677–96. doi:10.1080/00218464.2012.751526.

Taib, Abdelaziz A., Rachid Boukhili, Said Achiou, Sebastien Gordon, and Hychem Boukehili. 2006. “Bonded Joints with Composite Adherends. Part I. Effect of Specimen Configuration, Adhesive Thickness, Spew Fillet and Adherend Stiffness on Fracture.” *International Journal of Adhesion and Adhesives* 26 (4): 226–36. doi:10.1016/j.ijadhadh.2005.03.015.

Tang, Huaqing, and Longquan Liu. 2018. “A Novel Metal-Composite Joint and Its Structural Performance.” *Composite Structures* 206 (June). Elsevier: 33–41. doi:10.1016/j.compstruct.2018.07.111.

Valenza, Antonino, Vincenzo Fiore, and Livan Fratini. 2011. “Mechanical Behaviour and Failure Modes of Metal to Composite Adhesive Joints for Nautical Applications.” *International Journal of Advanced Manufacturing Technology* 53 (5–8): 593–600. doi:10.1007/s00170-010-2866-1.

Zal, Vahid, Hassan Moslemi Naeini, Ahmad Reza Bahramian, and Hadi Abdollahi. 2017. “Evaluation of the Effect of Aluminum Surface Treatment on Mechanical and Dynamic Properties of PVC/Aluminum/Fiber Glass Fiber Metal Laminates.” *Proceedings of the Institution of Mechanical Engineers, Part E: Journal of Process Mechanical Engineering* 231 (6): 1197–1205. doi:10.1177/0954408916657371.